scientific reports

OPEN

In vitro generation of transplantable insulin-producing cells from canine adipose-derived mesenchymal stem cells

Quynh Dang Le[1,2,4], Watchareewan Rodprasert[2], Suryo Kuncorojakti[2,3], Prasit Pavasant[6,8], Thanaphum Osathanon[6,7] & Chenphop Sawangmake[2,4,5,8]✉

Canine mesenchymal stem cells (cMSCs) have potential applications for regenerative therapy, including the generation of insulin-producing cells (IPCs) for studying and treating diabetes. In this study, we established a useful protocol for generating IPCs from canine adipose mesenchymal stem cells (cAD-MSCs). Subsequently, in vitro preservation of pluronic F127-coated alginate (ALGPA)-encapsulated cAD-MSC-derived IPCs was performed to verify ready-to-use IPCs. IPCs were induced from cAD-MSCs with the modulated three-stepwise protocol. The first step of definitive endoderm (DE) induction showed that the cooperation of Chir99021 and Activin A created the effective production of *Sox17*-expressed DE cells. The second step for pancreatic endocrine (PE) progenitor induction from DE indicated that the treatment with taurine, retinoic acid, FGF2, EGF, TGFβ inhibitor, dorsomorphin, nicotinamide, and DAPT showed the significant upregulation of the pancreatic endocrine precursor markers *Pdx1* and *Ngn3*. The last step of IPC production, the combination of taurine, nicotinamide, Glp-1, forskolin, PI3K inhibitor, and TGFβ inhibitor, yielded efficiently functional IPCs from PE precursors. Afterward, the maintenance of ALGPA-encapsulated cAD-MSC-derived IPCs with VSCBIC-1, a specialized medium, enhanced IPC properties. Conclusion, the modulated three-stepwise protocol generates the functional IPCs. Together, the encapsulation of cAD-MSC-derived IPCs and the cultivation with VSCBIC-1 enrich the maturation of generated IPCs.

Diabetes mellitus (DM) is a complex metabolic disorder characterized by a chronic presence of hyperglycemia and glycosuria as the results of insulin deficiency or impaired insulin response to target tissues[1–3]. DM is one of the common endocrine diseases diagnosed in the canine family besides human beings[4]. An epidemiological study in the United States reported a 32 percent increase in canine diabetes between 2006 and 2011, and the data kept on rising by 47.7 percent from 2011 to 2016[5]. By pathophysiological diagnosis, canine DM has been mostly concerned with beta cell deficiency by latent autoimmunity, which is considered as similar with human type 1 DM (T1DM)[6,7]. Insulin therapy has been clinically well-established to manage T1DM in both dogs and humans, however, adverse events and disadvantages have also been periodically reported[8–10]. In 2000, a trial of islet transplantation was performed successfully according to "Edmonton protocol", thus this method introduced as an alternative approach for treating long-term hyperglycemia with insulin independence[11–13]. Although pancreatic islet transplantation can surmount the impediments of insulin therapy, the lack of donor islet source and the immune reactivity of recipients exist as two main obstacles of this method[11,12,14]. To solve the restrictions

[1]International Program of Veterinary Science and Technology, Faculty of Veterinary Science, Chulalongkorn University, Bangkok, Thailand. [2]Veterinary Stem Cell and Bioengineering Innovation Center (VSCBIC), Veterinary Pharmacology and Stem Cell Research Laboratory, Faculty of Veterinary Science, Chulalongkorn University, Bangkok, Thailand. [3]Department of Veterinary Science, Faculty of Veterinary Medicine, Universitas Airlangga, Surabaya, East Java, Indonesia. [4]Veterinary Stem Cell and Bioengineering Research Unit, Faculty of Veterinary Science, Chulalongkorn University, Bangkok, Thailand. [5]Department of Pharmacology, Faculty of Veterinary Science, Chulalongkorn University, Bangkok, Thailand. [6]Department of Anatomy, Faculty of Dentistry, Chulalongkorn University, Bangkok, Thailand. [7]Dental Stem Cell Biology Research Unit, Faculty of Dentistry, Chulalongkorn University, Bangkok, Thailand. [8]Center of Excellence in Regenerative Dentistry (CERD), Faculty of Dentistry, Chulalongkorn University, Bangkok, Thailand. ✉email: chenphop.s@chula.ac.th

of the Edmonton protocol, the tendency of regenerative medicine production in which insulin-producing cells (IPCs) derived from stem cells has been a promising candidate[12,15].

Current in vitro IPCs are generated by embryonic stem cells (ESCs), induced pluripotent stem cells (iPSCs) and mesenchymal stem cells (MSCs). Nevertheless, ESCs have encountered ethical issues, while reprogramming of iPSCs can cause teratoma formation and side effects of pluripotency-induced viral transgenes might be unsafe for clinical applications[16]. Meanwhile, MSCs possess immune-privileged and highly plastic abilities, this allows MSCs to be a wonderful and safe choice for IPC generation[16]. The capacity of human MSCs (hMSCs) differentiated into IPCs as well as their clinical accomplishment has been shown in many previous studies[17–20]. Although a minority of research on IPCs has originated from canine MSCs (cMSCs)[21–23], these cMSC-derived IPCs are still functionally inadequate and morphologically circumscribed. To fabricate the effective cMSC-derived IPCs, it is essential to advance the current differentiation protocols. In types of cMSCs, canine adipose-derived MSCs (cAD-MSCs) are an accessible candidate and possess the potency for IPC differentiation[22,23]. Therefore, this study focused on establishing a protocol for cAD-MSCs induction toward mature IPCs in vitro. Moreover, preservation of cAD-MSC-derived IPCs, which were encapsulated in alginate gel and pluronic acid (ALGPA) following our previous study[24], would also be investigated. This knowledge will aid the fundamental insights for in vitro cAD-MSC-derived IPC generation and eventually for in vivo transplantation study.

Results

Isolation and characterization of cAD-MSCs.
cAD-MSCs showed adherent-dependent and fibroblast-like cells on the 2 dimensions (2D) culture (Fig. 1A). The mRNA expression of stemness markers (*Oct4* and *Rex1*) and proliferative marker (*Ki67*) were detected by RT-qPCR (Fig. 1B). In addition, MSC-related surface markers using flow cytometry revealed the strong expression of CD29 and CD90, moderate expression of CD44, low expression of CD73, but absent expression of CD45 (Fig. 1C).

Moreover, in vitro multi-differentiation potential toward adipogenic, osteogenic, and chondrogenic lineages was observed. cAD-MSCs dramatically upregulated adipogenic-related genes (*Leptin* and *LPL*) while the production of lipid droplets was detected by Oil Red O staining (Fig. 1D). Regarding osteogenic differentiation, the substantial upregulation of *Runx2* and *Ocn* was indicated upon exposed cells in osteogenic induction medium and osteocyte-produced calcium deposits were recognized by Alizarin Red S staining (Fig. 1E). For chondrogenic differentiation, the upregulation of the *Col2a1* gene was significantly disclosed, and glycosaminoglycan accumulation was stained with Alcian blue (Fig. 1F).

Thus, the isolated cAD-MSCs show homogeneous appearance and the differentiation potential toward other cell lineages.

Cooperation of GS3K inhibitor Chir99021 with Activin A enhances definitive endoderm formation from cAD-MSCs.
First, formation of definitive endoderm (DE), a germ cell layer, is an essential initiation step for giving rise to pancreatic cells[25,26]. DE were generated from cAD-MSCs using DE induction media supplemented with Activin A alone for 72 h (protocol 1.1; P.1.1) or Chir99021 for first 24 h and following with Activin A for 48 h (protocol 1.2; P.1.2) (Fig. 2A). Small three-dimension (3D) clusters were formed from dissociated cAD-MSCs cultured in suspension for 24 h, then size and density of colonies were increased (Fig. 2B). On day 3, the total colony counts (medium) were 1610.75 and 1637.25 colonies per batch (1×10^6 seeding cells) in P.1.1 and P.1.2 groups, respectively (Fig. 2C). Interestingly, the distribution of size-based colonies showed that the small-to-medium colony size (100–299 µm) occupied the most population in both protocols, and P.1.2 yielded significantly more medium-size colonies (300–499 µm) than P.1.1 (Fig. 2D).

Levels of mRNA expression related to mesendoderm (ME) and DE were analyzed and compared to undifferentiated cells. The ME-related markers (*Eomes* and *GSC*) in P.1.2 showed the upregulated expression in a time-dependent manner (Fig. 2E). In contrast, the expression of *Mixl1* was upregulated in P.1.1, while P.1.2 was downregulated. For the DE-related markers, both protocols upregulated all genes comparing with undifferentiated control (Fig. 2F). However, P.1.2 was able to increase the expression of *Gata4*, *Gata6*, and *Sox17* on the last day of DE induction.

Generally, the result revealed that the cooperation of Chir99021 and Activin A is effectively on the generation of DE from cAD-MSCs with small-size and the crucial DE-related markers.

Combination of signaling modulators systematically generates pancreatic endocrine precursors.
Pancreatic endocrine (PE) stage is the vital second stage on pancreatic development process according to its important roles in cell fate modulation on DE cell toward pancreatic cell types[27,28]. In this part, three established protocols were explored; protocol 2.1 (P.2.1), protocol 2.2 (P.2.2), and protocol 2.3 (P.2.3) (Fig. 3A). All protocols exposed the 3D floating colonies which became bigger and denser along the culture period (Fig. 3B). All protocols showed the similar trend of total colony count, however, there were gently decreasing by the induction day (Fig. 3C). For the sized-based colony number, the number of colonies was mostly found in 100–299 µm, nevertheless, the large-size colonies were slightly increasing during the induction period (Fig. 3D).

Except for the *Glut2* gene, the expression of other mRNA markers relating to the development of PE precursors exhibited significant differences among the protocols. Compared to the undifferentiated cells and DE cells on day 3, the expression of pancreatic endoderm marker (*Pdx1*) was upregulated in groups treated with P.2.2 and P.2.3 on day 5 and day 8, while there was not detected in P.2.1 (Fig. 4A). The expression of *Hnf1b*, *Hnf4a*, and *Hnf6*, known as primitive gut and posterior foregut markers, was upregulated on day 5 and day 8 post-induction in P.2.2 and P.2.3 (Fig. 4B). The multipotent pancreatic progenitor (MPP) marker (*Ptf1a*) was upregulated on day 5 in three protocols, however, the trend of *Ptf1a* downregulation was found in P.2.2 and P.2.3 on day 8 (Fig. 4C). On other hand, P.2.2 and P.2.3 exhibited the upregulation trend of the other MPP markers (*Sox9* and *Nkx6.1*)
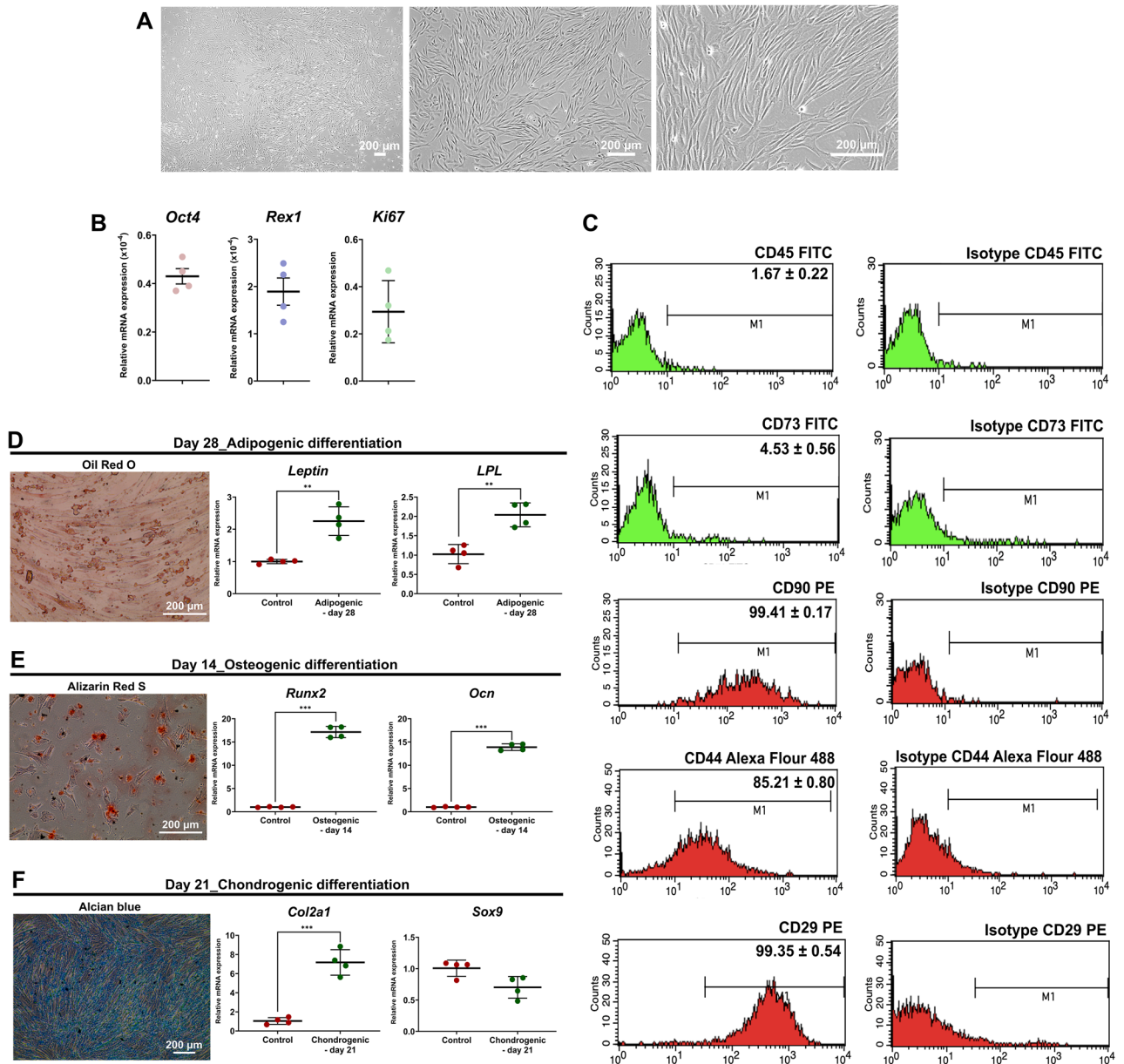
Figure 1. cAD-MSC characteristics. Morphological appearances of cAD-MSCs were observed under a light microscope with magnification of 4X, 20X, and 40X (**A**). The mRNA expression of stemness markers (*Oct4*, and *Rex1*) and a proliferation marker (*Ki67*) were analyzed by RT-qPCR (**B**), normalized with the reference gene (*Gapdh*). Expression of surface markers exhibiting MSC property were revealed using flow cytometry (**C**). Adipogenic differentiation potential at day 28 post-induction was stained with Oil Red O, and adipogenic related-mRNA expression was determined (**D**). Osteogenesis was confirmed using Alizarin Red S staining at day 14 post-induction, and the expression of osteogenic mRNA markers were assessed (**E**). Chondrogenic differentiation potential at day 21 post-induction was demonstrated by Alcian blue staining, and chondrogenic mRNA markers were determined (**F**). The expression of mRNA genes related to multilineage differentiation was normalized with the reference gene and the undifferentiation control. Bars indicates the significant differences (**, p value <0.01, ***, p value <0.001).

on the last day of PE induction (Fig. 4C). All of the protocols showed the increased expression of the PE-related mRNA markers such as *Nkx2.2*, *Pax4*, *Ngn3*, *NeuroD1*, and *Isl1* on day 8, compared to undifferentiated cells (Fig. 4D). On day 8, it is noticed that the highest expression of *Nkx2.2* and *NeuroD1* was found in P.2.1, whereas the greatest expression of *Ngn3*, a master key for endocrine specification, was found in P.2.3. In addition, the immature pancreatic endocrine marker, *MafB*, was tremendously upregulated in P.2.2 and P.2.3 on day 8 compared to the undifferentiated cells (Fig. 4E). Moreover, P.2.2 and P.2.3 displayed the significant downregulation of *Hes1*, Notch target gene, on the last day of PE induction (Fig. 4F). Besides, compared with cAD-MSCs, P.2.1 increased the expression of *Cdkn1a*, a cell cycle regulator, on day 8, while the decreased expression was observed in P.2.2 and P.2.3 (Fig. 4G).
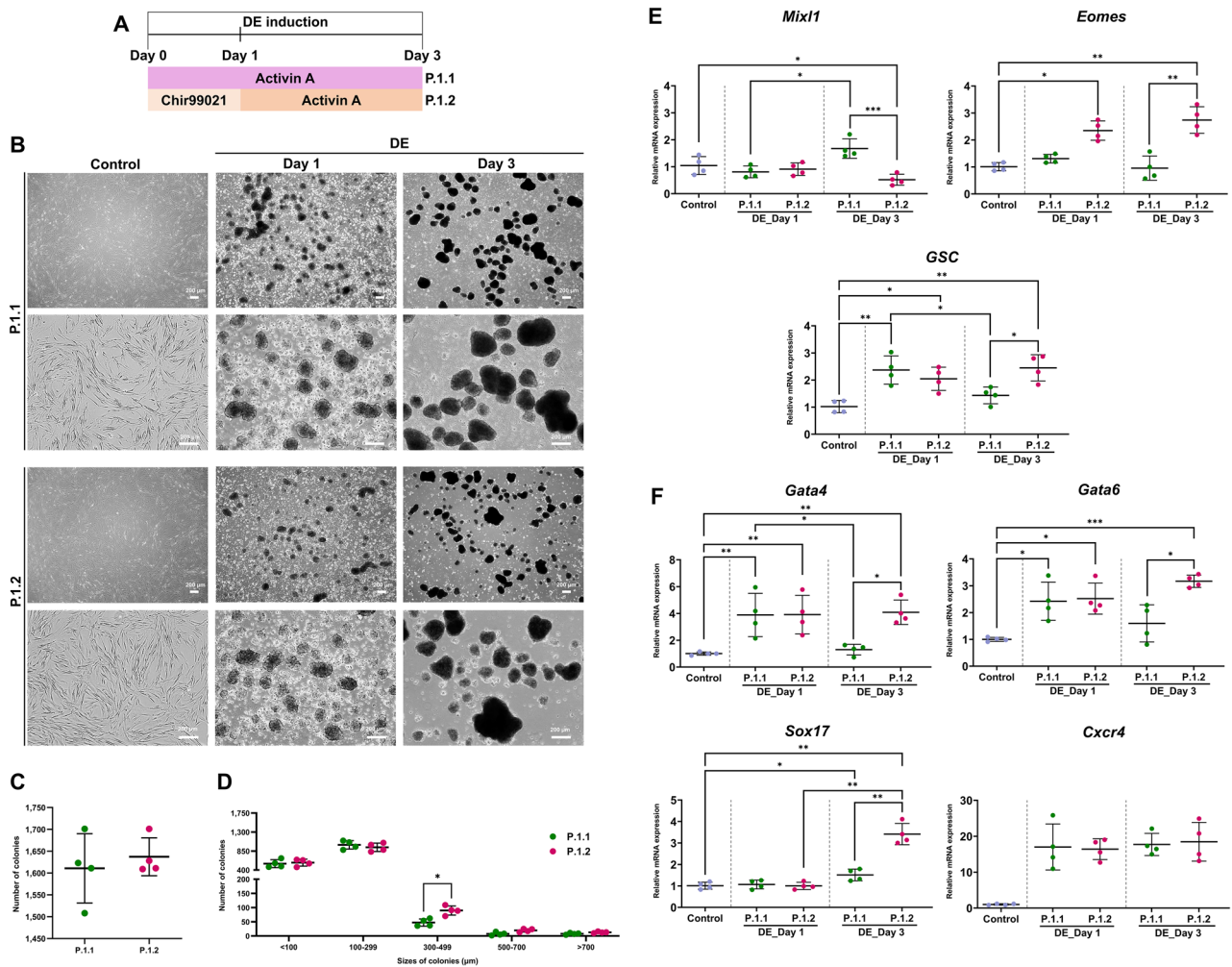
Figure 2. Generation of cAD-MSC-derived DE cells. The diagrams of two protocols used for the induction of cAD-MSC derived DE cells are shown in (**A**). Differentiation of morphological appearances of cAD-MSCs toward DE cells was observed at day 1, and 3 (**B**). The total colony number (**C**) and the distribution of colony sizes (**D**) were evaluated. The expression of mRNA markers relating to mesendoderm status (**E**), and definitive endoderm status (**F**) was analyzed by RT-qPCR at day 1, and 3 post-induction. Relative mRNA expression was normalized with the reference gene, and the undifferentiation control. Bars indicates the significant differences (*, p value < 0.05; **, p value < 0.01; ***, p value < 0.001).

Regarding all the results, the new combination of signaling modulators supports the PE development. Importantly, the obtained PE cells from P.2.3 showed the greatest PE-related mRNA expression.

Combination of forskolin, PI3K inhibitor, and TGFβ inhibitor enriches the functional maturation of IPCs.

Last induction, two cocktail media were established to effectively induce functional IPCs from PE precursors; formulas of protocol 3.1 (P.3.1) and protocol 3.2 (P.3.2) are defined in Fig. 5A. Therefore, PE colonies on day 8 were encapsulated in alginate gels, then the encapsulated PE were induced toward IPCs. Both protocols were still showing a 3D colony morphology during IPC induction period (Fig. 5B).

Except for *Nkx6.1* gene, the mRNA expression of PE progenitor-related markers (*Pdx1*, *NeuroD1*, *Isl1*, *Ngn3*, and *Glut2*) was upregulated in P.3.2, compared to undifferentiated cells and PE cells on day 8 (Fig. 5C). Conversely, the downregulation trend of *Nkx6.1*, *NeuroD1*, *Isl1* was found in P.3.1 compared to PE cells (Fig. 5C). The expression of mature endocrine markers, including *Glis3*, *MafA*, *Insulin*, and *Glucagon*, was upregulated in both of protocols, compared with those from undifferentiation cells and PE cells (Fig. 5D). However, the highest expression of mature endocrine markers was explored in P.3.2. Furthermore, P.3.2 showed the upregulation of hormone release-related markers (*Epac2* and *Rfx6*), compared to undifferentiated cells and PE cells (Fig. 5E). Although P.3.1 showed the trend of increasing *Rfx6* expression, the downregulation of *Epac2* was found in this protocol (Fig. 5E).

At day 13 of IPC induction, cAD-MSC-derived IPCs in both P.3.1 and P.3.2 were further evaluated the functional potential regarding the production of C-peptide upon glucose stimulation at two different concentrations, 5.5 mM and 22 mM. The findings showed that IPCs in both the protocols yield C-peptide under a basal condition, the higher production of C-peptide was found in P.3.2 (Fig. 6A). Moreover, IPCs from P.3.2 secreted C-peptide
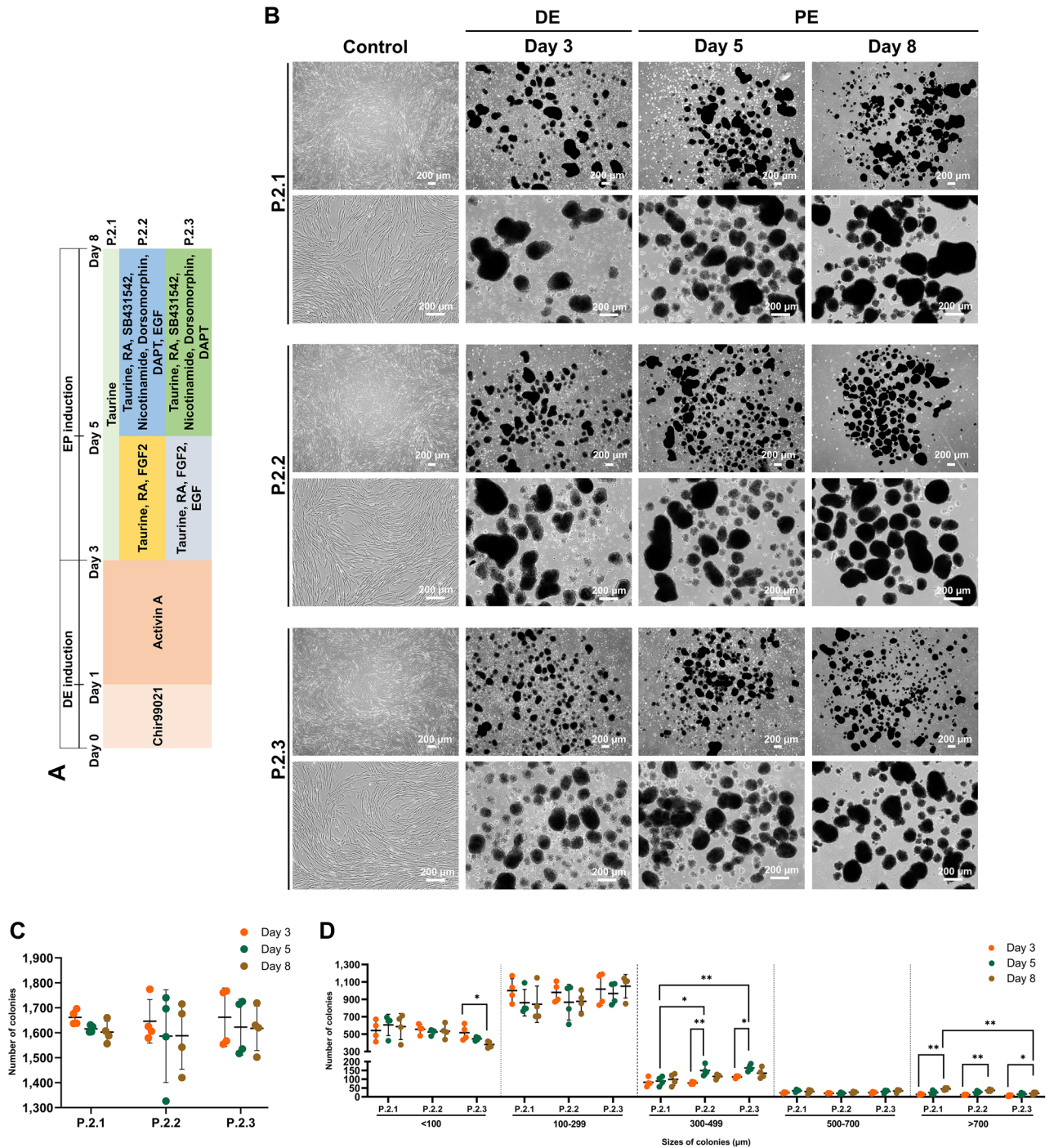
Figure 3. Generation of cAD-MSC-derived PE cells. The diagrams of three protocols used for the induction of cAD-MSC-derived PE cells are shown in (**A**). Differentiation of morphological appearances of cAD-MSCs toward PE cells was observed at day 3, 5 and 8 (**B**). The total colony number (**C**) and the distribution of colony sizes (**D**) were evaluated. Bars indicates the significant differences (*, *p* value < 0.05; **, *p* value < 0.01).

in concentration-dependent manner upon high (22 mM) glucose stimulation, compared to those from basal control and P.3.1 (Fig. 6A). In addition, immunocytochemistry staining was employed to confirm the expression of the crucial pancreatic islet-related hormones, Insulin and Glucagon. The result suggested that the expression of these proteins was observed on cAD-MSC-derived IPCs in both protocols on day 13 post-induction (Fig. 6B).

Taken together, the results suggested that P.3.2 which used forskolin, PI3K inhibitor, and TGFβ inhibitor could have more positive effects on IPCs' maturation from cAD-MSC-derived PE cells.
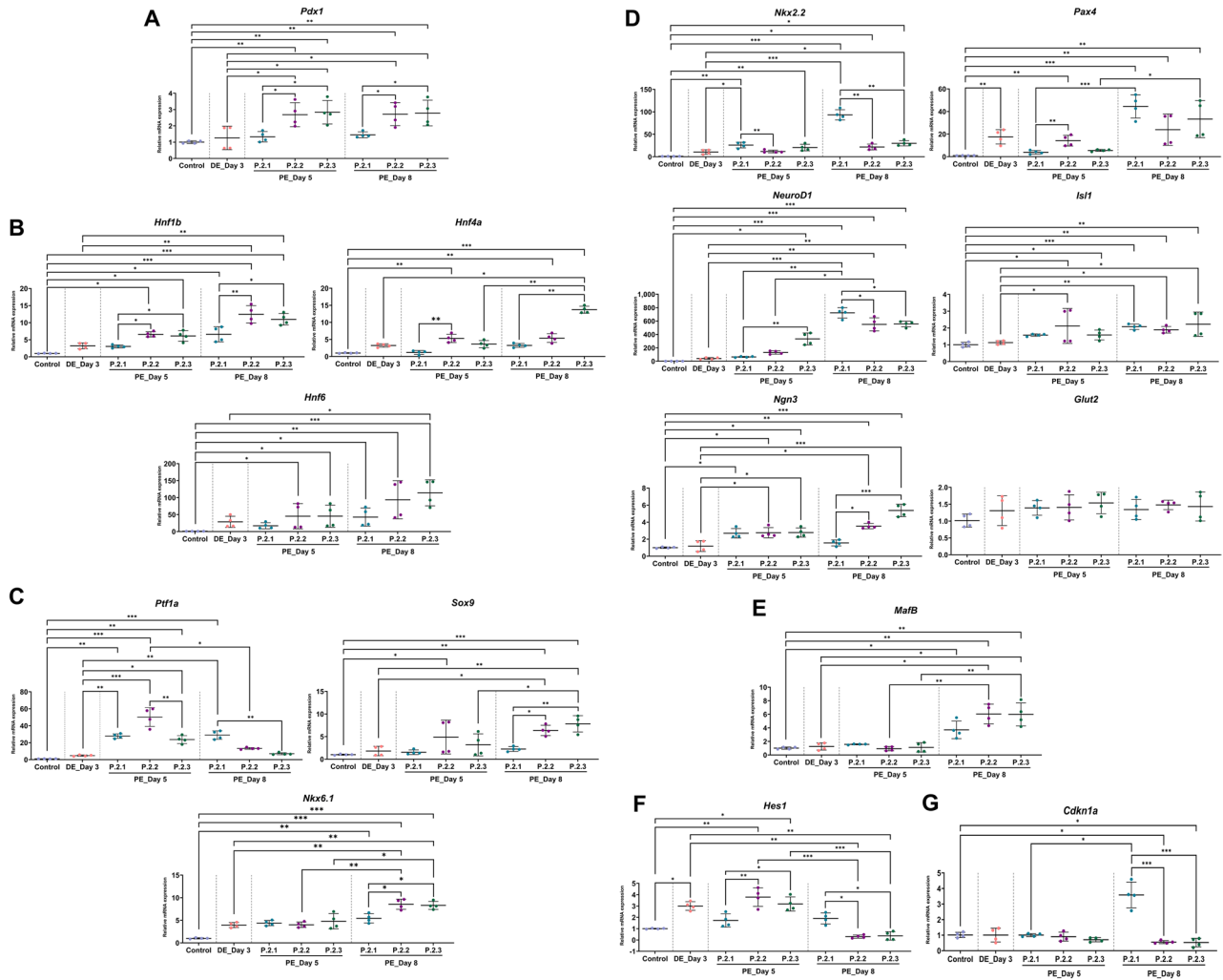
Figure 4. PE-related marker expression. The expression of mRNA markers relating to pancreatic endoderm (**A**), primitive gut and posterior foregut (**B**), pancreatic multipotent progenitor (**C**), endocrine precursors (**D**), immature pancreatic endocrine (**E**), caNotch pathway target gene (**F**), and a cell cycle regulator (**G**) was analyzed by RT-qPCR at day 3, 5 and 8 post-induction. Relative mRNA expression was normalized with the reference gene, and the undifferentiation control. Bars indicates the significant differences (*, p value < 0.05; **, p value < 0.01; ***, p value < 0.001).

Nourishment of specialized medium, VSCBIC-1, on ALGPA-encapsulated IPC's sustenance. It is essential to generate ready-to-use (RTU) IPCs for in vivo application. Maintenance of ALGPA-encapsulated cAD-MSC-derived IPCs in vitro is required. Hence, three different media were chosen to maintain the ALGPA-encapsulated cAD-MSC-derived IPCs in vitro after 13 days of IPC induction process (Fig. 7A). Medium 4.1 (M.4.1) is normal DMEM, medium 4.2 (M.4.2) is an IPC induction medium (P.3.2), and medium 4.3 (M.4.3) is VSCBIC-1, our specialized medium[29]. PE progenitors on day 8 would be double encapsulated in ALGPA instead of only alginate. Morphological changes were observed for 2 weeks after 13 days of IPC induction process (Fig. 7B). Damaged IPCs were not found in ALGPA, but the colonies became smaller in all three media. All maintenance media showed the viability of ALGPA-encapsulated cAD-MSC-derived-IPCs until day 27 by live/death staining (Fig. 7C). The mass of non-viable cells was detected in all three media along the maintenance period. In addition, cAD-MSC-derived IPCs on day 27 in M.4.2 and M.4.3 exhibited the upregulation trend of PE mRNA markers (*Nkx6.1*, *Pdx1*, *Isl1*, and *Glut2*) compared IPCs from day 13 and IPCs from M.4.1 (Fig. 8A). Although the decreasing of *Ngn3* and *NeuroD1* was found in all media compared with IPCs on day 13, M.4.3 showed the insignificant decline (Fig. 8A). Interestingly, the increasing of *Nkx2.2* was showed in M.4.1 (Fig. 8A). In other hand, the upregualtion of mature endocrine markers (*Glis3*, *MafA*, *Insulin*, *Glucagon*, and *Glp1r*) and hormone release-related markers (*Epac2*, and *Rfx6*) was explored in M.4.2 and M.4.3 compared with undifferentiated cells, IPCs from day 13, and IPCs from M.4.1 (Fig. 8B,C). Although the proliferation marker, *Ki67*, of IPCs was lower expressed in M.4.2 and M.4.3 than M.4.1, the upregulation of a cell cycle regulator, *Cdkn1a,* was found in M.4.2 and M.4.3 groups (Fig. 8D,E).

The functional property was evaluated by the level of C-peptide secretion (Fig. 8F). The result showed the trend of concentration-dependent response upon 22 mM glucose stimulation in M.4.2 and M.4.3 groups, while
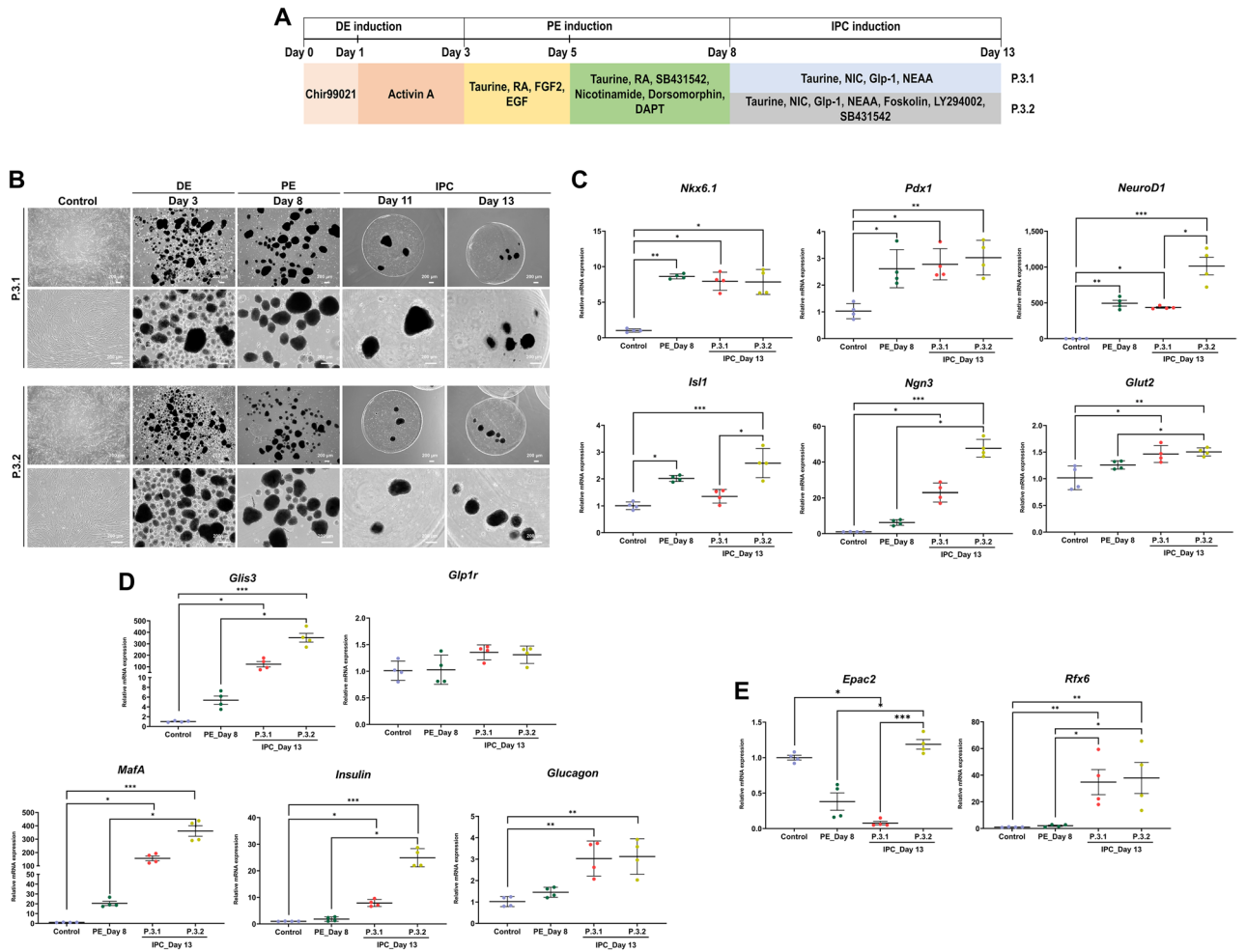
Figure 5. Generation of cAD-MSC-derived IPCs. The diagrams of two protocols used for the induction of cAD-MSC derived IPCs are shown in (**A**). Differentiation morphological appearances of cAD-MSCs toward IPCs were observed at day 8 and 13 post-induction (**B**). The expression of mRNA markers relating to PE precursors (**C**), mature endocrine progenitors (**D**), hormone release-related markers (**E**). Relative mRNA expression was normalized with the reference gene, and the undifferentiation control. Bars indicates the significant differences (*, p value < 0.05; **, p value < 0.01; ***, p value < 0.001).

M.4.1 exhibited the releasing of C-peptide level response to 5.5 mM glucose stimulation. Additionally, the protein expression of Insulin and Glucagon was done using immunocytochemical staining. The result confirmed that both hormones were detected in all maintenance media (Fig. 8G).

According to the results, the utilization of VSCBIC-1 reveals the preservation effect of ALGPA-encapsulated cAD-MSC-derived IPCs together with the maturation of produced IPCs.

Discussion

The concept of stem cell therapy holds gigantic promise for treating diabetes[30], MSCs provide an auspicious platform to produce clinically applicable IPCs[31–37]. In this study, cAD-MSC induction protocol toward mature IPCs and the enriched medium for preserving AGLPA-encapsulated cAD-MSC-derived IPCs were established to produce RTU IPCs. The cAD-MSCs were isolated, cultured, and expanded following our previous report[38]. These isolated cAD-MSCs were then defined following the International Society for Cellular Therapy (ISCT)[39], they presented fibroblast-like cell sharp, adherent to culture plastic. In addition, pluripotent markers *Oct4* and *Rex1* were expressed, which reflects the multipotent and proliferative properties[40,41]. Furthermore, MSCs were required to exhibit CD73, CD90, CD44, and CD29 surface markers, and lack expression of CD45 marker[39]. Similar to our result, other previous studies also illustrated low expression of CD73 on various types of cMSCs, even on MSCs of some other animals[42,43]. It is noted that CD73 expression could be different among various sources and species. Moreover, the isolated cells showed capacity toward adipogenic, chondrogenic, osteogenic differentiation as same as previous studies[41,44–48]. All these evidences reflect the potential and homogeneity of the isolated cAD-MSCs.

Currently, various differentiation protocols of IPCs were published[49–54]. The strategies of these protocols were established on ESCs and iPSCs. Although ESC-derived IPCs have achieved positive outcomes of insulin-secreting
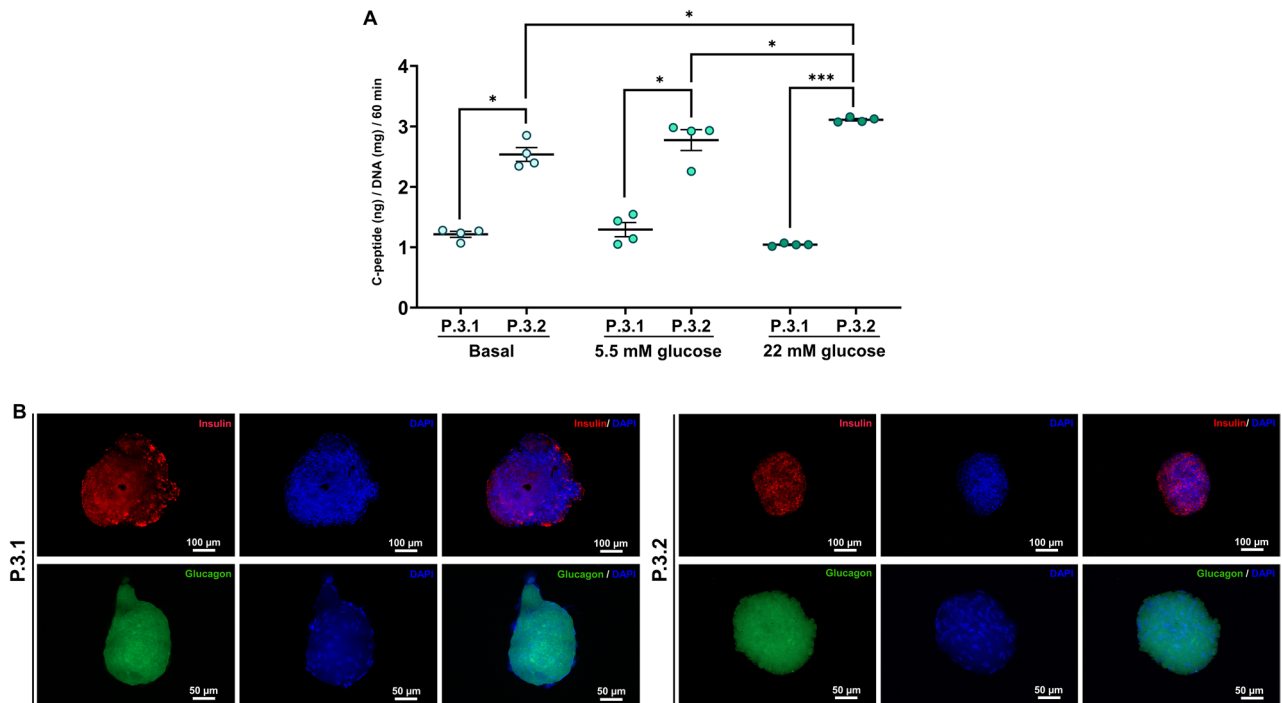
Figure 6. Functionality of cAD-MSC-derived IPCs. C-peptide secretion was determined by glucose-stimulated C-peptide secretion (GSCS) assay (**A**). The expression of Insulin and Glucagon by cAD-IPCs was detected by immunocytochemistry on day 13 by immunocytochemistry and observed under fuorescent microscope ZEISS Apotome.2 (Carl Zeiss, Germany) incorporated with Axio Observer Z1 and ZEN pro sofware (ZEISS International, Germany) at 10X (Insulin) and 20X (Glucagon) (**B**). Bars indicates the significant differences (*, p value < 0.05; ***, p value < 0.001).

regulation in clinical trials[55,56], ESCs are acrimoniously encountering with ethical issues[55–57]. Alternatively, iPSCs, which are generated from somatic cells, are promoted due to avoiding from the ethics and resolving MSC's drawbacks[58]. Nevertheless, iPSCs need to overcome other challenges, including tumorigenicity, and genetic instability[59,60]. In 2020, Adrian et al. conducted the generation of good manufacturing practice (GMP)-grade iPSC-MSCs for using in clinical trials, which overcame the risk of teratoma formation by a filtration process[61]. However, almost cell reprogramming is often made using viral vectors which is a serious concern[62–64], and the simpler and cost-effective method is required for preventing teratoma formation[65]. Compared to ESCs and iPSCs, adult tissue-MSCs are inherently restricted by imperfect capacity of proliferation and weakened differentiation capacity with prolonged culture and high passage number[66,67], but MSCs are exempted from the ethical limitations and iPSC's restrictions. Furthermore, MSCs are widely used in clinical trials[68], thus MSCs are offered as a good candidate for IPC generation[16]. The MSC-based protocols mainly comprise of three differentiation stages[16,38,69–71]. The different stages for MSCs are DE, PE progenitors, and IPC maturation. Although IPCs could be produced from cAD-MSCs with the simple three-stepwise protocol[69,70], their function is still hamperred[38]. Here, we illustrated that the modified three-stepwise protocol could improve the in vitro functional IPC differentiation from cAD-MSCs.

As the first step of IPC-derived MSCs, DE formation is a prerequisite for generating efficient pancreatic lineage from MSCs[72]. In previous studies, Activin A and Chir99021 were known as the potential small molecules on DE development[38,69,70,73]. Although the independent utilization of Chir99021 and Activin A could induce DE from stem cells[74–77], the cooperation of Chir99021 and Activin A could optimize for inducing DE cells[76,77]. Here, Chir99021, a strong indirect activator of the canonical Wnt-pathway via inhibition of GSK3β signaling pathway, allows MSCs differentiate into ME, a mesendoderm lineage[76,77]. Subsequently, DE is induced from ME by treating with Activin A which is known as an endogenous noggin[25,26,73,78]. The cascade of ME specification before DE is considered as physiologically relevant[79]. Previous studies found that at ME stage, the cells expressed *Mixl1*, *Eomes*, and *GSC* and at DE stage expressed *Gata4/6*, *Sox17*, and *Cxcr4*, meanwhile the roles of these markers are modulating the cell's decision deriving to ME and DE states[63,80–84]. Therefore, in various previous research, the expression of *Mixl1*, *Eomes*, *GSC*, *Gata4/6*, *Sox17* and *Cxcr4* transcripts was used as crucial markers to confirm the ME and DE cells[76,77]. In this study, we analyzed the expression of these transcript markers to assess the ME and DE formation of both protocols. Our findings showed that the expression of ME markers, *Eomes* and *GSC*, was found the significant upregulation after treating Chir99021 for 24 h. The later generation of DE was defined by Activin A through the upregulated expression of *Sox17*, *Gata4*, *Gata6*. Together, these results demonstrated that Chir99021 synergizes Activin A to effectively generate DE cells from cAD-MSCs.

Next, DE cells from previous step were induced into PE cells. Importantly, PE progenitors represent a critical step of in vitro IPC differentiation[85,86]. In natural pancreatic development, it is required the development of DE into primitive gut, posterior foregut, and PE precursors, respectively[85–87]. Our study found that the combination of
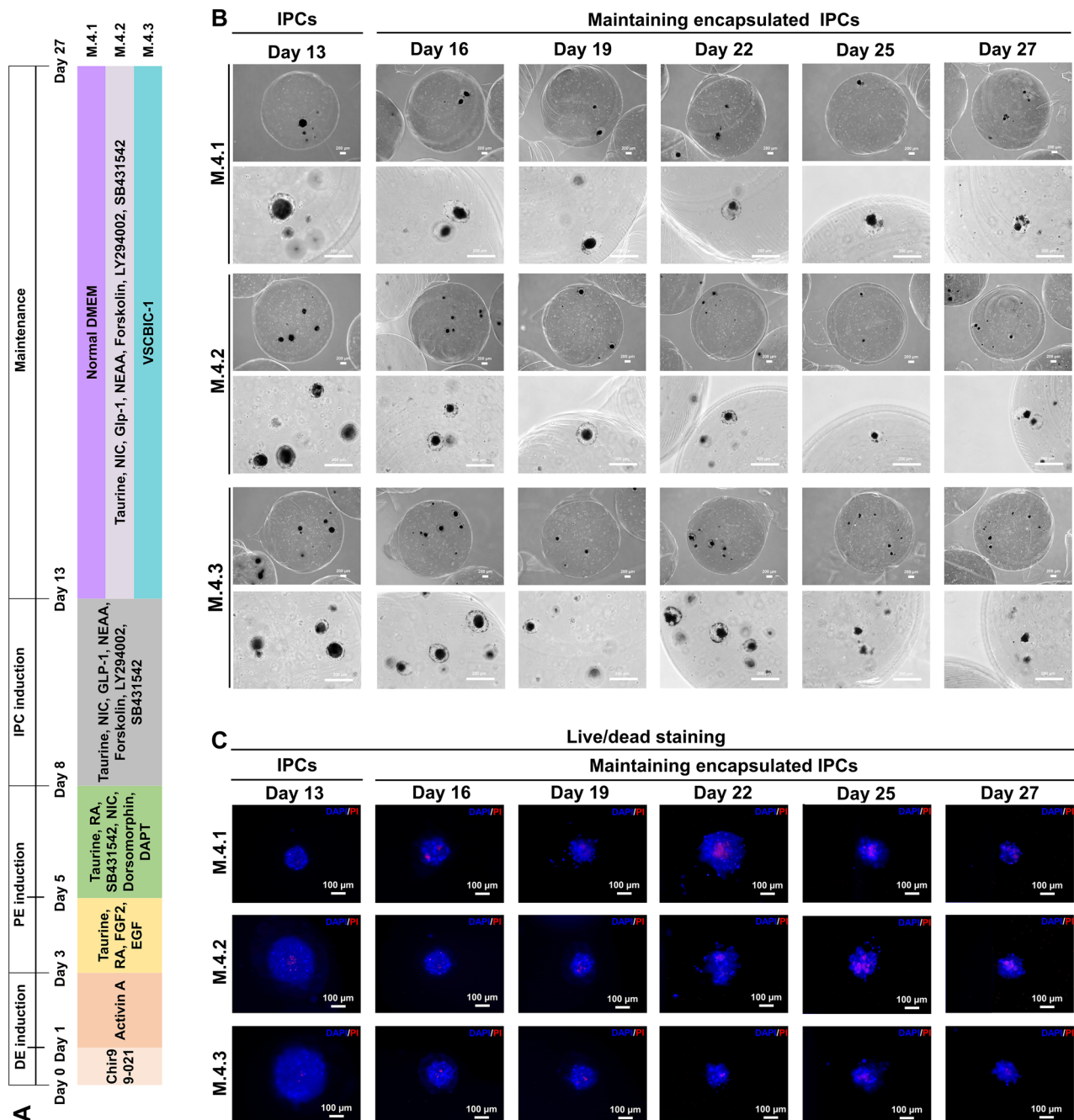
Figure 7. Morphological and viability evaluation of ALGPA-encapsulated cAD-MSCs-derived IPCs. The cAD-MSC-derived IPC induction diagram and media maintaining IPCs encapsulated in ALGPA are shown in (**A**). ALGPA-encapsulated cAD-MSCs-derived IPCs' morphological appearances were observed at day 13, 16, 19, 22, 25, and 27 post induction (**B**). The viability evaluation of encapsulated cAD-MSC-derived IPCs was determined by live/dead staining (**C**).

small molecules in PE induction medium, which consisted of taurine, retinoic acid (RA), FGF2, EGF, SB431542, dorsomorphin, nicotinamide (NIC), and DAPT, show the positive outcome, especially P.2.3. Here, the group treated with taurine alone revealed the hasty differentiation by the greater expression of endocrine percursor markers (*Nkx2.2*, *Pax4*), however, they showed the lowest expression of *Pdx1* and *Nkx6.1*, pancreatic endoderm and multipotent progenitor markers, which could cause the undesired commitments of the cell's fates[88,89]. It is noticed that EGF, epidermal growth factor, could promote the proliferation of *Sox9*/*Pdx1*-positive pancreatic progenitors[90]. We found that the using of EGF in early pancreatic differentiation (P.2.3) resulted the most efficient induction of Ngn3-positive PE precursors, while the using of EGF in late pancreatic differentiation stage (P.2.2) confined the differentiation of Ngn3-positive PE cells. Previous study reported that the presence of EGF was able to repress the differentiation of PE cells[91]. In several research on vertebrates, the important role of RA in pancreatic developments were detailly described[92,93], while FGF2, a factor of notochord, is required to initiate
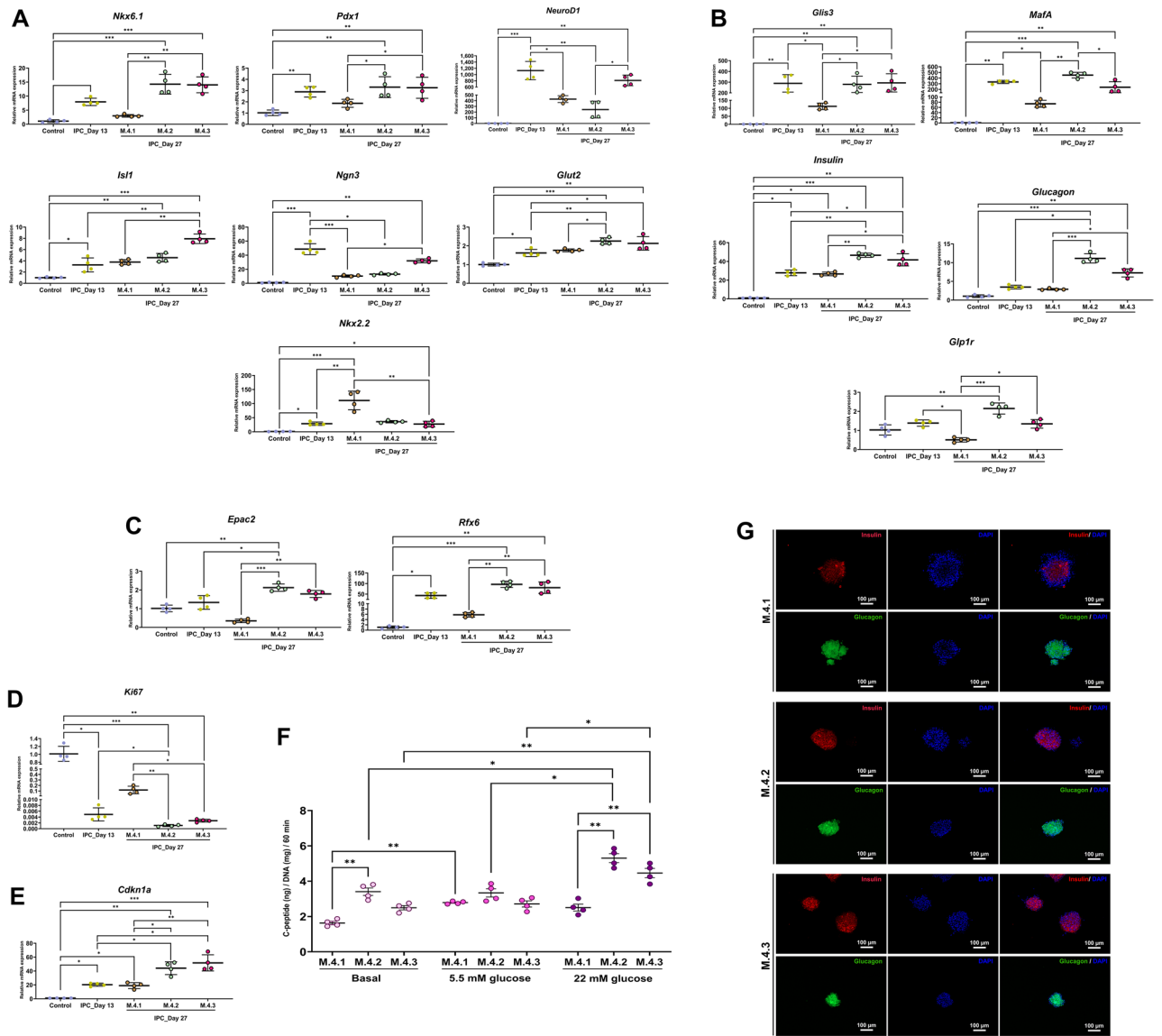
Figure 8. Sustainable functionality of VSCBIC-1 on ALGPA-encapsulated cAD-MSCs-derived IPC maintenance. The expression of mRNA markers relating to PE precursors (**A**), mature endocrine progenitors (**B**), hormone-releasing markers (**C**), a proliferation marker (**D**), and a cell cycle regulator (**E**) was analyzed by RT-qPCR at day 27 post-induction. C-peptide secretion was determined by glucose-stimulated C-peptide secretion (GSCS) assay (**F**). The expression of Insulin and Glucagon by cAD-IPCs was detected on day 27 by immunocytochemistry and observed under fuorescent microscope ZEISS Apotome.2 (Carl Zeiss, Germany) incorporated with Axio Observer Z1 and ZEN pro sofware (ZEISS International, Germany) (**G**). Relative mRNA expression was normalized with the reference gene, and the undifferentiation control. Bars indicates the significant differences (*, p value < 0.05; **, p value < 0.01; ***, p value < 0.001).

for pancreatic development by inhibiting Shh expression[94–96]. Our result also defines the role of RA and FGF2 in the early pancreatic development by showed the increased expression of the primitive gut and posterior foregut markers (*Hnf1b*, *Hnf4a*, *Hnf6*) and pancreatic endoderm marker (*Pdx1*). Combination of RA, dorsomorphin, and SB431542 achieved the effective commitment on Pdx1-positive cell induction[75]. Also, another previous study showed that the cocktail including EGF, BMP inhibitor, and NIC boosted the induction of *Nkx6.1*, another crucial regulator of pancreatic islet development[97]. DAPT, known as an inhibitor of Notch signaling pathway, directly represses the expression of *Hes1* (Notch targeted gene)[98]. Transcription of *Hes1* gene inhibits the promotion of *Ngn3* gene[99], while *Ngn3* expression is essentially required for endocrine cell development[98]. Our previous studies proved that the inhibition of Notch signaling during PE induction benefits IPC generation from MSCs[38,69]. Although RA could also suppress the *Hes1* expression indirectly[93], further analyses are still required. BMP antagonism dorsomorphin inhibited Smad1/5/8 phosphorylation to expand the levels of *Ins* expression, which affected the production of essential hormone "Insulin" in β-cell development process[100,101]. Moreover, the inhibitor of TGFβ type I receptor, SB431542, also promotes the increased the expression of *Ins*[101]. Interestingly, our discovery revealed that the upregulation of *Sox9*, *Nkx6.1*, *Pax4*, *NeuroD1*, *Isl1*, and *Ngn3* was found by

combined treatment with RA, SB431542, dorsomorphin, NIC, and DAPT. Furthermore, our study also found that a modified medium P.2.3 restricted the expression of *Cdkn1a*, a cell cycle regulator, during PE induction process. *Cdkn1a* was known that it plays a critical role in the cellular mediation by the overexpression of *Cdkn1a* results in cell cycle arrest[102]. Therefore, the suppression of this marker means the proliferative ability of IPCs. However, the further evaluation is still required. In summary, cAD-MSC-derived PE progenitors could be enriched when cAD-MSC-derived DE cells were treated with the combination of taurine, RA, FGF2, and EGF for 2 days, and then the mixture of taurine, RA, SB431542, dorsomorphin, NIC, and DAPT for 3 days.

Regarding the natural pancreatic development, PE cells can give rise to all types of pancreatic islets (alpha, beta, delta, epsilon, and upsilon)[85–87]. Therefore, the generation of islet β-like cells, which can secrete insulin responding to glucose stimulation, is the aim of in vitro IPC induction[33,85–87]. Unfortunately, cAD-MSC-derived PE colonies tend to lose their shape and decrease their number after the PE induction process (not shown data), this problem was also found in a previous study[103]. Meanwhile, the entrapment of 3D-PE organoids not only maintains their shapes, but also improves their differentiation property and hormone synthesis[103–106]. Hence, cAD-MSC-derived PE colonies were encapsulated in alginate gel before they were induced to IPCs. In this study, the functional IPC generation was found when PE precursors were treated with the mixture of taurine, NIC, Glp-1, NEAA, forskolin, LY294002, and SB431542. Forskolin and Glp-1 play important roles in insulin releasing process via the membrane adenylate cyclase (AC) cascade to covert ATP to cAMP, then modulate insulin secretion via PKA and PKC pathway. Forskolin directly stimulates AC, while Glp-1 will stimulate after the binding to its receptor[107–109]. Moreover, the inhibition of SB431542 via the TGFβ/ALK5 pathway could induce the expression of *MafA* and *NeuroD1* because of the upregulation of Foxo1 protein[108]. The inhibition of phosphoinositide 3-kinases (PI3K)/AKT pathway, LY290042, also potentiates the functional maturation of IPCs[51,110]. Here, *MafA*, *Insulin*, and *Glucagon* were the essential markers for islet maturation[111], while *Glut2, Epac2* and *Rfx6* were reported to increase the IPC-related hormone secretion capacity[107–109,112,113]. Interestingly, we found that the expression of *MafA*, *Insulin*, *Glucagon*, *Glut2, Epac2* and *Rfx6* was upregulated in cAD-MSC-derived IPCs treated with P.3.2 (the combination of taurine, NIC, Glp-1, NEAA, forskolin, LY294002, and SB431542). Subsequently, the trend of concentration-dependent response upon 22 mM glucose stimulation was also discovered. Moreover, the higher expression of *Ngn3* was found on day 13 compared to PE at day 8, thus this cocktail, named "P.3.2" could stimulate the production of PE precursors alongside the mature IPCs. Hence, the IPCs on day 13 contained not only mature IPCs but also *Ngn3*-expressing PE cells, the similar results were also found in earlier studies[114–116]. These evidences indicate that cAD-MSC-derived PE can be more likely to undergo differentiation into IPCs by treatment with the combination of taurine, NIC, Glp-1, NEAA, forskolin, LY294002, and SB431542.

According to our previous study, although cAD-MSCs showed as the potential MSC candidate for IPC generation from a simple three-stepwise induction protocol and low attachment culture technique, the trend of glucose-responsive C-peptide secretion upon high (22 mM) glucose stimulation was not found different compared to normal (5.5 mM) glucose condition[38]. In this study, we improved the three-stepwise induction protocol through establishing the new microenvironment manipulation of each step. Interestingly, our modified induction protocol showed the improvement of cAD-MSCs-derived IPC generation. The trend of concentration-dependent response upon high (22 mM) glucose was notably superior compared to basal and normal (5.5 mM) conditions which reflects the glucose sensing of generated IPCs. Therefore, IPCs from the modified protocol may show sufficient function for improving hyperglycemic state in vivo.

The entrapment of IPCs in alginate not only maintains 3D-floating colony shape, but also enhances differentiation and hormone synthesis[103–106]. Besides, the aims of encapsulation are to immobilize the implants as well as build a wall from the body's immune system for in vivo application[117]. Several previous studies were reported that the encapsulation of pancreatic islet, IPCs from ESCs and iPSCs using alginate could maintain the viability and functionality both in vivo and in vitro[53,104,105,118–120]. However, a greatest obstacle of monolayer capsule is the protrusion of cells. Our previous study showed that ALGPA-encapsulated hDPSC-derived IPCs can be preserved their viability and functionality[24]. Thus, ALGPA encapsulation may solve protrusion of IPCs and create favorable conditions for clinical treatments. In this study, we hypothesized that the in vitro preservation of ALGPA-encapsulated cAD-MSC-derived IPCs can provide the availability of IPCs for in vivo application requirements.

Here, three media were employed to investigate the preservation of ALGPA-encapsulated cAD-MSC-derived IPCs; M.4.1 (normal DMEM), M.4.2, and M.4.3 (VSCBIC-1). The specialized medium, VSCBIC-1, could maintain the morphology, viability, and functionality of mouse islets[29]. In addition, VSCBIC-1 could resuscitate the impaired islets derived from gut leak-induced IL-10 knockout mice[29]. Excitingly, the result showed that VSCBIC-1 could help to preserve viability of the outer cells in colonies after 13 days of IPC induction. In contrast, we found mass of non-viable cells in the core of encapsulated IPC colonies that was correlated to our previous study[24]. Additionally, we analyzed the expression of *Cdkn1a* which could activate anti-apoptosis and response to DNA damage or metabolic stress for supporting the cell survival[121,122], and the better upregulation of *Cdkn1a* was found in VSCBIC-1.

Moreover, VSCBIC-1 improved functionality of ALGPA-encapsulated cAD-MSC-derived IPCs. Interestingly, the maintained upregulation of *Ngn3* was also found in VSCBIC-1. Likewise, it has been reported that taurine, an essential amino acid, affects the pancreas development, enhances and maintains the endocrine function, and increases the size and number of the islets[123]. Also, NIC, a form of vitamin B, acts as a poly (ADP-ribose) polymerase inhibitor that is used to promote MSCs homing functional PE/IPCs and preserve the islet viability and function by protection of NAD^+/NADH ratio[117,124]. Thus, both taurine and NIC are used during differentiation into PE/IPCs and in vitro preservation. Which both small molecules were contained in both M.4.2 and M.4.3. On other hand, our observations suggested that the long-term induction with forskolin, LY294002, and SB431542, resulted in over-maturation of cAD-MSCs-derived IPCs as the extremely higher expression of markers in regard to IPC's maturation, the lower expression of *Ngn3* and the tremendously highest C-peptide secretion were detected on day 27 post-induction.

Briefly, VSCBIC-1 medium preserves the colonies in both PE and premature/mature IPC statuses until day 14 since the last day of the IPC induction, while the IPCs in P.4.2 medium were seemingly found in mature IPC status. Additionally, the colony population in VSCBIC-1, which contains both PE and premature/mature IPCs, is suitable for transplantation with the following reasons. First, in vitro generated PE/premature IPCs would get more maturation after transplantation[125–130]. Second, PE cells could be able to take a longer than mature IPCs for achieving the reversed hyperglycemia in DM patients due to the prolonged maturation period in vivo[129,131–133]. Third, downregulation of *Ki67* from IPCs in VSCBIC-1 indicated that the proliferation is inhibited, this might be safe for transplantation because of restricted invasion capacity[134–136]. Fourth, the ability on releasing insulin/C-peptide upon high glucose stimulation was still responded when they were maintained in VSCBIC-1. Moreover, a lower expression of HLA on hESC-derived PE/premature IPCs permits maintenance of immune privilege[137], this also indicated that PE/premature IPCs are more suitable for transplantation. Taken together, the potential of VSCBIC-1 medium is not only in preservation of IPCs, but also in production of RTU cAD-MSC-derive IPCs.

Conclusion

Briefly, we established the three-stepwise protocol for generating IPCs from cAD-MSCs for 13 days. Combined management of small molecules could induce proficient differentiation into DE, PE precursors and IPCs. Our findings suggested that cAD-MSC-derived IPCs could be well-generated with our modified protocol. Moreover, these present results approved that the viability and functionality of ALGPA-encapsulated cAD-MSC-derived IPCs can be preserved for 14 days in specialized medium VSCBIC-1. For the further study, in vivo study is required to evaluate the safety and potential of clinical application of ALGPA-encapsulated cAD-MSC-derived IPCs.

Materials and methods

cAD-MSC isolation and culture.   All procedures were conducted in compliance with the ARRIVE guidelines and according to regulations approved by the Institutional Animal Care and Use Committee (IACUC), Faculty of Veterinary Science, Chulalongkorn University (Animal Use Protocol No. 1531072). According to the inclusion criteria, four healthy dogs aged from 10 months to 5 years old were recruited (all dogs weighted over 5 kg) with their owner's consent. Each of cAD-MSC line, which was collected from each donor dog (n = 4), was used in this study. Briefly, biopsied adipose tissues were collected from abdominal fat after anesthesia by veterinarians at Small Animal Hospital, Chulalongkorn University. cAD-MSCs were isolated following our previous study[38], and they were reserved in the cell inventory for this study. In brief, adipose explants were washed twice with Phosphate Buffer Saline (PBS, Thermo Fisher Scientific Corporation, USA) before they minced and incubated in Cell Recovery Solution (Corning, USA) for 2 h at 37 °C. Then, the mixture was passed through the Falcon 70 μm Cell Strainer (Corning). Cells were collected by centrifuge at 2000 rpm for 5 min, and then resuspended and cultured onto T-75 flasks (Corning) contained Dulbecco's Modified Eagle Medium (DMEM, Thermo Fisher Scientific) under 37 °C, 5% CO_2 in humidified environment. The medium was supplemented with 10% Fetal Bovine Serum (FBS, Thermo Fisher Scientific), 1% GlutaMAX™ (Thermo Fisher Scientific), and 1% Antibiotic–Antimycotic (Thermo Fisher Scientific). Cells were subcultured once 80% confluence was reached. Cells at passage 3–5 were used for all experiments.

Characterization and multilineage differentiation potential assay.   cAD-MSCs were characterized by cell morphology under a phase-contrast microscope, and mRNA expression relating to stemness markers (*Oct4* and *Rex1*) and a proliferation marker (*Ki67*) by RT-qPCR. Besides, MSC-related surface markers were analyzed by flow cytometry. In particular, the cells were stained with FITC-conjugated mouse anti-human CD45 antibody (BioLegend, USA), mouse anti-human CD73 monoclonal antibody (Thermo Fisher Scientific) and FITC-conjugated goat anti-mouse immunoglobulin G (IgG) secondary antibody (BioRad, USA), PE-conjugated rat anti-dog CD90 monoclonal antibody (eBioscience, USA), Alexa Fluor 488-conjugated rat anti-dog CD44 antibody (BioRad), PE-conjugated mouse anti-human CD29 monoclonal antibody (Bio Legend). FITC-conjugated mouse IgG1 kappa Isotype (BioLegend), mouse IgG2a kappa Isotype (Thermo Fisher Scientific), PE-conjugated rat IgG2b kappa Isotype (eBioscience), Alexa Fluor 488-conjugated rat IgG2a Isotype (BioRad), PE-conjugated mouse IgG1 kappa Isotype (BioLegend) were used as isotype controls. The results were analyzed using a FACScalibur flow cytometer with CellQuest software (BD Bioscience, USA).

Differentiation potentials of cAD-MSCs were investigated using adipogenic, osteogenic, and chondrogenic induction protocols according to our previous study[41,69,138].

For adipogenic differentiation, 3×10^4 cAD-MSCs were seeded onto a 24-well culture plate and treated with adipogenic induction medium supplemented with 10% FBS, 0.1 mg/mL insulin (Sigma), 1 μM dexamethasone, 1 mM 3-isobutyl-1-methylxanthine (IBMX, Sigma), and 0.2 mM indomethacin (Sigma) for 28 days[41,69,138]. Afterwards, the intracellular lipid droplets were detected with Oil Red O (Sigma) staining and the expression of adipogenic mRNA markers (*Leptin*, and *LPL*) was assessed by RT-qPCR.

For osteogenic differentiation, cAD-MSCs (2.5×10^5 cells/well) were seeded onto 24-well culture plate (Corning) and induced with osteogenic induction medium contained DMEM supplemented with 10% FBS, 50 mg/mL ascorbic acid (Sigma, USA), 100 mM dexamethasone (Sigma), and 10 mM β-glycerophosphate (Sigma) for 14 days[69]. Extracellular matrix (ECM) mineralization was detected using Alizarin Red S (Sigma) dye. Osteogenic mRNA markers (*Runx2* and *Ocn*) were determined by RT-qPCR.

For chondrogenic differentiation, cAD-MSCs were induced in chondrogenic induction medium comprised of 15% FBS, 0.1 μM dexamethasone, 50 mg/mL L-ascorbic-2–2-phosphate (AA2P, Sigma), 4 mg/mL L-proline (Sigma), 2% antibiotic–antimycotic, and 10 ng/mL transforming growth factor (TGF)-β3 (Sigma), and 1% insulin-transferrin-selenium (ITS, Thermo Fisher Scientific) for 21 days[41,69,138]. Subsequently, glycosaminoglycan

formation was detected by Alcian Blue (Sigma) staining and the expression of chondrogenic mRNA markers (*Sox9* and *Col2a1*) was evaluated by RT-qPCR.

In vitro insulin-producing cell differentiation. The protocol of insulin-producing cell (IPC) induction was separated into three main stages including definitive endoderm (DE), pancreatic endocrine progenitors (PEP), and insulin-producing cells (IPCs). All induction media were using DMEM as the basal media which were not adding any FBS, called "serum-free media (SFM)".

For DE induction, cells were collected by trypsinization and centrifuge at 2000 rpm, 4 °C for 5 min. Then, a million of cells was induced into DE with 2 different protocols. In P.1.1, the cells were cultured in SFM-1.1 supplemented with 1% ITS, 1% BSA (Cohn fraction V, fatty acid free, Sigma), 4 nM Activin A (Sigma), and 1 nM sodium butyrate (Sigma) for 3 days. In P.1.2, the cells were cultured SFM-1.2 supplemented with DMEM supplemented with 1% BSA, 4 nM Chir99021 (Sigma), and 1 nM sodium butyrate for a day before changing to SFM-1.1 for 2 days.

For PE precursor induction, DE clusters were induced into PE with 3 different protocols. In P.2.1, SFM-2.1 contained 1% BSA, 1% ITS, and 0.3 mM taurine (Sigma) was utilized for 5 days. In P.2.2, DE clusters were cultured in SFM-2.2.1 supplemented with 1% BSA, 1% ITS, 0.3 mM taurine, and 20 ng/mL bFGF (Sigma) for 2 days, then the medium was changed to SFM-2.2.2 which was supplemented with 1% BSA, 1% ITS, 0.3 mM taurine, 2 μL retinoic acid (RA, Sigma), 10 mM nicotinamide (Sigma), 25 μL DAPT (Sigma), 1 μL dorsomorphin (Sigma), 10 μL SB431542 (Sigma) and 50 ng/mL EGF (Sigma) for 3 days. In P.2.3, DE clusters were culture in SFM-2.3.1 supplemented with 1% BSA, 1% ITS, 0.3 mM taurine, 20 ng/mL bFGF and 50 ng/mL EGF for 2 days, then the medium was replaced by SFM-2.3.2 contained 1% BSA, 1% ITS, 0.3 mM taurine, 2 μM RA, 10 mM nicotinamide, 25 μL DAPT, 1 μM dorsomorphin, and 10 μM SB431542, and cultured for 3 days.

When the PE induction protocol was verified, PE cells were continually differentiated toward IPCs after they were encapsulated with alginate gel (Sigma). Two different protocols were utilized to induce PE cells to IPCs for 5 days. P.3.1 was made by DMEM supplemented with 1% BSA, 1% ITS, 3 mM taurine, 1 mM nicotinamide, 100 nM glucagon-like peptide-1 (GLP-1, Sigma), and 1% non-essential amino acids (NEAA, Sigma). P.3.2 was supplemented 1% BSA, 1% ITS, 3 mM taurine, 1 mM nicotinamide, 100 nM GLP-1, 1% NEAA, 10 μM SB431542, 10 μL forskolin (Sigma), and 10 μM LY294002 (Sigma).

Encapsulation. The protocol of colony encapsulation was followed by a previous report[24], cAD-MSC-derived colonies were harvested and resuspended in 2% alginate solution. Sterile polystyrene syringe and 22G needle (Nipro, Japan) were used to generate alginate beads. Drops of beads were collected in 100 mM CaCl$_2$ (Sigma-Aldrich) under stirring conditions, and then washed by Krebs–Ringer- Hepes (KRH) containing CaCl$_2$ buffer. For double-layer encapsulation, a cold solution of 30% pluronic F127 was added to cover all surfaces of alginate beads at room temperature (RT).

Maintenance of the alginate/Pluronic acid-encapsulated IPC's function in vitro. Subsequently of IPC induction, three different media were applied to consider the maintenance ability of the IPCs' function and viability in vitro. M.4.1 is basic DMEM with 10% FBS. M.4.2 is an IPC induction medium (P.3.2). M.4.3 is VSCBIC-1 which was prepared following our previous study[29].

Reverse transcription quantitative polymerase chain reaction (RT-qPCR). The total cellular RNA was extracted using TRIzol™ reagent (Thermo Fisher Scientific) and Direct-zol™ RNA Miniprep kit (Zymo Research, USA) according to the manufacturer's protocol. Successively, the cDNA was obtained from RNA using ImProm-II™ Reverse Transcription System (Promega, USA). Targeted genes were amplified and detected by FastStart Essential DNA Green Master (Roche Diagnostics, USA) and CF96™ real-time PCR detection system (BioRad). The mRNA expression was illustrated as relative mRNA expression by normalized to Glyceraldehyde 3-phosphate dehydrogenase (*Gapdh*) and the undifferentiated cells as a control. The $2^{-\Delta\Delta t}$ formula was used to calculate relative gene expression. All primers were designed by NCBI primer designing tool based on the mRNA sequences from NBCI database (https://www.ncbi.nlm.nih.gov). The primers sequences and their accession number are shown in Supplementary Table S1.

Immunocytochemistry (ICC). IPC colonies were fixed in cold methanol for 15 min at RT, then permeabilized with 0.1% Triton-X100 (Sigma). After that, the background was blocked with 10% donkey serum for 1 h. The primary antibodies, rabbit anti-insulin (Cell signature technology, USA)[139] at dilution 1:200 and mouse anti-rat glucagon (Abcam, USA)[140] at dilution 1:200, were added and incubated overnight. Then, cyanine (Cy) 3-conjugated donkey anti-rabbit IgG (Bio Legend) and FITC-conjugated goat anti-mouse IgG (BioRad) were used as secondary antibodies, respectively. After incubation with secondary antibodies for 2 h, DAPI was used to stain the nucleus. The results and images were acquired using a fluorescent microscope ZEISS Apotome.2 (Carl Zeiss, Germany) incorporated with Axio Observer Z1 and ZEN pro software (ZEISS International, Germany).

Functional test and enzyme-linked immunosorbent assay (ELISA). The IPCs were assessed the function by glucose-stimulated C-peptide secretion assay (GSCS)[24,38,69,70,138]. The IPCs were incubated in normal KRH bicarbonate (KRBH) buffer (pH 7.4) for 1 h as basal control, then in 5.5 mM of glucose anhydrous (Sigma) in KRBH for the next 1 h and finally in 22 mM glucose anhydrous in KRBH for 1 h. Enzyme-linked immunosorbent assay (ELISA) kit (Millipore) was used for detecting the generated C-peptide level according to the manufacturer's protocol. Total DNA (ng) and stimulation time (mins) were used to normalization.

Live/dead staining. Encapsulated IPCs were evaluated for their viability using the NUCLEAR-ID Blue/Red cell viability reagent (GFP-CERTIFIED) (Enzo Life Science, USA), according to the manufacturer's protocol. The result was clarified under a fluorescent microscope (ZEISS Apotome.2 (Carl Zeiss, Germany) incorporated with Axio Observer Z1 and ZEN pro software (ZEISS International, Germany).

Statistical analyses. The total number of colony and their size distribution were determined using ImageJ software and standardized with hemocytometer square size from 10 randomly positions. The results were illustrated by a dot plot (n = 4) using GraphPad Prism 9.0 (Graph Software Inc., San Diego, CA). SPSS Statistics 22 software (IBM Corporation, USA) was employed to analyze the results. The Mann–Whitney U test was exercised to compare two independent groups, while the Kruskal–Wallis was devoted to analyze three or more experimental groups. Statistically, a significant difference was considered as a p-value < 0.05.

Data availability

The RT-qPCR gene expression data has been deposited to the Gene Expression Omnibus (GEO) repository under accession number GSE196118. The other generated and analyzed datasets during the current study are available from the corresponding author upon reasonable request.

References

1. Kharroubi, A. T. & Darwish, H. M. Diabetes mellitus: The epidemic of the century. *World J. Diabetes* **6**, 850–867. https://doi.org/10.4239/wjd.v6.i6.850 (2015).
2. Punthakee, Z., Goldenberg, R. & Katz, P. Definition, classification and diagnosis of diabetes, prediabetes and metabolic syndrome. *Can. J. Diabetes* **42**(Suppl 1), S10-s15. https://doi.org/10.1016/j.jcjd.2017.10.003 (2018).
3. Schmidt, A. M. Highlighting diabetes mellitus: The epidemic continues. *Arterioscler. Thromb. Vasc. Biol.* **38**, e1–e8. https://doi.org/10.1161/atvbaha.117.310221 (2018).
4. Niaz, K. *et al.* Comparative occurrence of diabetes in canine, feline, and few wild animals and their association with pancreatic diseases and ketoacidosis with therapeutic approach. *Vet. World* **11**, 410–422. https://doi.org/10.14202/vetworld.2018.410-422 (2018).
5. Banfield Pet Hospital. State of Pet Health 2016 Report. 12–14 (2016).
6. Rand, J. S., Fleeman, L. M., Farrow, H. A., Appleton, D. J. & Lederer, R. Canine and feline diabetes mellitus: Nature or nurture?. *J. Nutr.* **134**, 2072s–2080s. https://doi.org/10.1093/jn/134.8.2072s (2004).
7. Nerhagen, S. & Mooney, C. T. Canine diabetes mellitus Diabetes mellitus is a common endocrinopathy in dogs and can be a frustrating disease to manage, both for the owner and the veterinarian, write (2017).
8. Handelsman, Y. *et al.* American association of clinical endocrinologists and American college of endocrinology—clinical practice guidelines for developing a diabetes mellitus comprehensive care plan—2015. *Endocr. Pract.* **21**(Suppl 1), 1–87. https://doi.org/10.4158/EP15672.GL (2015).
9. Kalra, S. *et al.* Hypoglycemia: The neglected complication. *Indian J. Endocrinol. Metab.* **17**, 819–834. https://doi.org/10.4103/2230-8210.117219 (2013).
10. Rivera, N. *et al.* Insulin-induced hypoglycemia increases hepatic sensitivity to glucagon in dogs. *J. Clin. Invest.* **120**, 4425–4435. https://doi.org/10.1172/jci40919 (2010).
11. Bruni, A., Gala-Lopez, B., Pepper, A. R., Abualhassan, N. S. & Shapiro, A. J. Islet cell transplantation for the treatment of type 1 diabetes: Recent advances and future challenges. *Diabetes Metab. Syndr. Obes.* **7**, 211–223. https://doi.org/10.2147/dmso.S50789 (2014).
12. Khosravi-Maharlooei, M. *et al.* THERAPY OF ENDOCRINE DISEASE: Islet transplantation for type 1 diabetes: So close and yet so far away. *Eur. J. Endocrinol.* **173**, R165-183. https://doi.org/10.1530/eje-15-0094 (2015).
13. Sekine, K. *et al.* Regenerative medicine approach as an alternative treatment to islet transplantation. *Transpl. Proc.* **44**, 1104–1106. https://doi.org/10.1016/j.transproceed.2012.03.020 (2012).
14. Lablanche, S. *et al.* Islet transplantation versus insulin therapy in patients with type 1 diabetes with severe hypoglycaemia or poorly controlled glycaemia after kidney transplantation (TRIMECO): A multicentre, randomised controlled trial. *Lancet Diabetes Endocrinol.* **6**, 527–537. https://doi.org/10.1016/s2213-8587(18)30078-0 (2018).
15. Pokrywczynska, M., Krzyzanowska, S., Jundzill, A., Adamowicz, J. & Drewa, T. Differentiation of stem cells into insulin-producing cells: Current status and challenges. *Arch. Immunol. Ther. Exp. (Warsz)* **61**, 149–158. https://doi.org/10.1007/s00005-012-0213-y (2013).
16. Manaph, N. P. A. *et al.* An overview on small molecule-induced differentiation of mesenchymal stem cells into beta cells for diabetic therapy. *Stem Cell Res. Ther.* **10**(293), 2019. https://doi.org/10.1186/s13287-019-1396-5 (2019).
17. Chandra, V. *et al.* Islet-like cell aggregates generated from human adipose tissue derived stem cells ameliorate experimental diabetes in mice. *PLoS ONE* **6**, e20615. https://doi.org/10.1371/journal.pone.0020615 (2011).
18. Gabr, M. M. *et al.* Insulin-producing cells from adult human bone marrow mesenchymal stem cells control streptozotocin-induced diabetes in nude mice. *Cell Transpl.* **22**, 133–145. https://doi.org/10.3727/096368912x647162 (2013).
19. Phadnis, S. M. *et al.* Human bone marrow-derived mesenchymal cells differentiate and mature into endocrine pancreatic lineage in vivo. *Cytotherapy* **13**, 279–293. https://doi.org/10.3109/14653249.2010.523108 (2011).
20. Xin, Y. *et al.* Insulin-Producing cells differentiated from human bone marrow mesenchymal stem cells in vitro ameliorate streptozotocin-induced diabetic hyperglycemia. *PLoS ONE* **11**, e0145838. https://doi.org/10.1371/journal.pone.0145838 (2016).
21. Brevini, T. A. *et al.* Epigenetic conversion of adult dog skin fibroblasts into insulin-secreting cells. *Vet. J.* **211**, 52–56. https://doi.org/10.1016/j.tvjl.2016.02.014 (2016).
22. Camara, B. O. S. *et al.* Differentiation of canine adipose mesenchymal stem cells into insulin-producing cells: Comparison of different culture medium compositions. *Domest. Anim. Endocrinol.* **74**, 106572. https://doi.org/10.1016/j.domaniend.2020.106572 (2021).
23. Teshima, T. *et al.* Generation of insulin-producing cells from canine adipose tissue-derived mesenchymal stem cells. *Stem Cells Int.* **2020**, 8841865. https://doi.org/10.1155/2020/8841865 (2020).
24. Kuncorojakti, S. *et al.* Alginate/Pluronic F127-based encapsulation supports viability and functionality of human dental pulp stem cell-derived insulin-producing cells. *J. Biol. Eng.* **14**, 23. https://doi.org/10.1186/s13036-020-00246-1 (2020).
25. Kubo, A. *et al.* Development of definitive endoderm from embryonic stem cells in culture. *Development* **131**, 1651–1662. https://doi.org/10.1242/dev.01044 (2004).

26. Shim, J. H. *et al.* Directed differentiation of human embryonic stem cells towards a pancreatic cell fate. *Diabetologia* **50**, 1228–1238. https://doi.org/10.1007/s00125-007-0634-z (2007).
27. Aigha, I. I. & Abdelalim, E. M. NKX6.1 transcription factor: A crucial regulator of pancreatic β cell development, identity, and proliferation. *Stem Cell Res. Ther.* **11**, 459. https://doi.org/10.1186/s13287-020-01977-0 (2020).
28. Arda, H. E., Benitez, C. M. & Kim, S. K. Gene regulatory networks governing pancreas development. *Dev. Cell* **25**, 5–13. https://doi.org/10.1016/j.devcel.2013.03.016 (2013).
29. Soedarmanto, A. *Recovery of Isolated Pancreatic Islet Derived from Gut Leak-induced Diabetes Type II Mouse Model.* Master thesis, Chulalongkorn, (2020).
30. Aggarwal, S. & Pittenger, M. F. Human mesenchymal stem cells modulate allogeneic immune cell responses. *Blood* **105**, 1815–1822. https://doi.org/10.1182/blood-2004-04-1559 (2005).
31. Betts, D. H. & Tobias, I. C. Canine pluripotent stem cells: Are they ready for clinical applications?. *Front. Vet. Sci.* **2**, 41. https://doi.org/10.3389/fvets.2015.00041 (2015).
32. Duan, W. & Lopez, M. J. Canine adult adipose tissue-derived multipotent stromal cell isolation and characterization. *Methods Mol. Biol.* **1773**, 189–202. https://doi.org/10.1007/978-1-4939-7799-4_16 (2018).
33. Gabr, M. M. *et al.* Insulin-producing cells from adult human bone marrow mesenchymal stromal cells could control chemically induced diabetes in dogs: A preliminary study. *Cell Transpl.* **27**, 937–947. https://doi.org/10.1177/0963689718759913 (2018).
34. Grohová, A., Dáňová, K., Špíšek, R. & Palová-Jelínková, L. Cell based therapy for type 1 diabetes: Should we take hyperglycemia into account?. *Front. Immunol.* **10**, 79. https://doi.org/10.3389/fimmu.2019.00079 (2019).
35. Hass, R., Kasper, C., Böhm, S. & Jacobs, R. Different populations and sources of human mesenchymal stem cells (MSC): A comparison of adult and neonatal tissue-derived MSC. *Cell Commun. Signal.* **9**, 12. https://doi.org/10.1186/1478-811X-9-12 (2011).
36. Lindner, U., Kramer, J., Rohwedel, J. & Schlenke, P. Mesenchymal stem or stromal cells: Toward a better understanding of their biology?. *Transfus. Med. Hemother.* **37**, 75–83. https://doi.org/10.1159/000290897 (2010).
37. Soria, B. *et al.* Insulin-secreting cells derived from embryonic stem cells normalize glycemia in streptozotocin-induced diabetic mice. *Diabetes* **49**, 157–162. https://doi.org/10.2337/diabetes.49.2.157 (2000).
38. Rodprasert, W. *et al.* Tailored generation of insulin producing cells from canine mesenchymal stem cells derived from bone marrow and adipose tissue. *Sci. Rep.* **11**, 12409. https://doi.org/10.1038/s41598-021-91774-3 (2021).
39. Dominici, M. *et al.* Minimal criteria for defining multipotent mesenchymal stromal cells. The International Society for Cellular Therapy position statement. *Cytotherapy* **8**, 315–317. https://doi.org/10.1080/14653240600855905 (2006).
40. Kolf, C. M., Cho, E. & Tuan, R. S. Mesenchymal stromal cells. Biology of adult mesenchymal stem cells: Regulation of niche, self-renewal and differentiation. *Arthritis Res. Ther.* **9**, 204. https://doi.org/10.1186/ar2116 (2007).
41. Nantavisai, S. *et al.* Simvastatin enhances proliferation and pluripotent gene expression by canine bone marrow-derived mesenchymal stem cells (cBM-MSCs) in vitro. *Heliyon* **5**, e02663. https://doi.org/10.1016/j.heliyon.2019.e02663 (2019).
42. Ivanovska, A. *et al.* Immunophenotypical characterization of canine mesenchymal stem cells from periviscer and subcutaneous adipose tissue by a species-specific panel of antibodies. *Res. Vet. Sci.* **114**, 51–58. https://doi.org/10.1016/j.rvsc.2017.02.019 (2017).
43. Nantavisai, S. *et al.* Systems biology analysis of osteogenic differentiation behavior by canine mesenchymal stem cells derived from bone marrow and dental pulp. *Sci. Rep.* **10**, 20703. https://doi.org/10.1038/s41598-020-77656-0 (2020).
44. Grzesiak, J., Marycz, K., Czogala, J., Wrzeszcz, K. & Nicpon, J. Comparison of behavior, morphology and morphometry of equine and canine adipose derived mesenchymal stem cells in culture. *Int. J. Morphol.* **29**, 1012–1017 (2011).
45. Kirkham, G. & Cartmell, S. Genes and proteins involved in the regulation of Osteogenesis. in *Topics in Tissue Engineering*, vol. 3 (2007).
46. Sasaki, A. *et al.* Canine mesenchymal stem cells from synovium have a higher chondrogenic potential than those from infrapatellar fat pad, adipose tissue, and bone marrow. *PLoS ONE* **13**, e0202922. https://doi.org/10.1371/journal.pone.0202922 (2018).
47. Sawangmake, C., Nantavisai, S., Osathanon, T. & Pavasant, P. Osteogenic differentiation potential of canine bone marrow-derived mesenchymal stem cells under different β-glycerophosphate concentrations in vitro. *Thai J. Vet. Med.* **46**, 617–625 (2016).
48. Teshima, T. *et al.* Comparison of properties of stem cells isolated from adipose tissue and lipomas in dogs. *Stem Cells Int.* https://doi.org/10.1155/2019/1609876 (2019).
49. Champeris Tsaniras, S. & Jones, P. M. Generating pancreatic beta-cells from embryonic stem cells by manipulating signaling pathways. *J. Endocrinol.* **206**, 13–26. https://doi.org/10.1677/joe-10-0073 (2010).
50. D'Amour, K. A. *et al.* Production of pancreatic hormone-expressing endocrine cells from human embryonic stem cells. *Nat. Biotechnol.* **24**, 1392–1401. https://doi.org/10.1038/nbt1259 (2006).
51. Hori, Y. *et al.* Growth inhibitors promote differentiation of insulin-producing tissue from embryonic stem cells. *Proc. Natl. Acad. Sci. U.S.A.* **99**, 16105–16110. https://doi.org/10.1073/pnas.252618999 (2002).
52. Tan, M., Jiang, L., Li, Y. & Jiang, W. Dual inhibition of BMP and WNT signals promotes pancreatic differentiation from human pluripotent stem cells. *Stem Cells Int.* **2019**, 5026793. https://doi.org/10.1155/2019/5026793 (2019).
53. Wang, N., Adams, G., Buttery, L., Falcone, F. H. & Stolnik, S. Alginate encapsulation technology supports embryonic stem cells differentiation into insulin-producing cells. *J. Biotechnol.* **144**, 304–312. https://doi.org/10.1016/j.jbiotec.2009.08.008 (2009).
54. Zhu, F. F. *et al.* Generation of pancreatic insulin-producing cells from rhesus monkey induced pluripotent stem cells. *Diabetologia* **54**, 2325–2336. https://doi.org/10.1007/s00125-011-2246-x (2011).
55. Li, G. *et al.* Generating mESC-derived insulin-producing cell lines through an intermediate lineage-restricted progenitor line. *Stem Cell Res.* **2**, 41–55. https://doi.org/10.1016/j.scr.2008.07.006 (2009).
56. Ramzy, A. *et al.* Implanted pluripotent stem-cell-derived pancreatic endoderm cells secrete glucose-responsive C-peptide in patients with type 1 diabetes. *Cell Stem Cell* **28**, 2047-2061.e2045. https://doi.org/10.1016/j.stem.2021.10.003 (2021).
57. Lo, B. & Parham, L. Ethical issues in stem cell research. *Endocr. Rev.* **30**, 204–213. https://doi.org/10.1210/er.2008-0031 (2009).
58. Lian, Q., Zhang, Y., Liang, X., Gao, F. & Tse, H. F. Directed differentiation of human-induced pluripotent stem cells to mesenchymal stem cells. *Methods Mol. Biol.* **1416**, 289–298. https://doi.org/10.1007/978-1-4939-3584-0_17 (2016).
59. Aboul-Soud, M. A. M., Alzahrani, A. J. & Mahmoud, A. Induced pluripotent stem cells (iPSCs)—roles in regenerative therapies, disease modelling and drug screening. *Cells* **10**, 2319 (2021).
60. Doss, M. X. & Sachinidis, A. Current challenges of iPSC-based disease modeling and therapeutic implications. *Cells* https://doi.org/10.3390/cells8050403 (2019).
61. Bloor, A. J. C. *et al.* Production, safety and efficacy of iPSC-derived mesenchymal stromal cells in acute steroid-resistant graft versus host disease: A phase I, multicenter, open-label, dose-escalation study. *Nat. Med.* **26**, 1720–1725. https://doi.org/10.1038/s41591-020-1050-x (2020).
62. Chen, K. G., Mallon, B. S., McKay, R. D. & Robey, P. G. Human pluripotent stem cell culture: Considerations for maintenance, expansion, and therapeutics. *Cell Stem Cell* **14**, 13–26. https://doi.org/10.1016/j.stem.2013.12.005 (2014).
63. Rojas, A. *et al.* Gata4 expression in lateral mesoderm is downstream of BMP4 and is activated directly by Forkhead and GATA transcription factors through a distal enhancer element. *Development* **132**, 3405–3417. https://doi.org/10.1242/dev.01913 (2005).
64. Singh, V. K., Kalsan, M., Kumar, N., Saini, A. & Chandra, R. Induced pluripotent stem cells: Applications in regenerative medicine, disease modeling, and drug discovery. *Front. Cell Dev. Biol.* **3**, 2. https://doi.org/10.3389/fcell.2015.00002 (2015).

65. Mohseni, R., Hamidieh, A. A., Verdi, J. & Shoae Hassani, A. Safe transplantation of pluripotent stem cell by preventing teratoma formation. *J. Stem Cell Res. Ther.* **4**, 1000212. https://doi.org/10.4172/2157-7633.1000212 (2014).
66. Li, O. *et al.* Human Embryonic stem cell-derived mesenchymal stroma cells (hES-MSCs) engraft in vivo and support hematopoiesis without suppressing immune function: Implications for off-the shelf ES-MSC therapies. *PLoS ONE* **8**, e55319. https://doi.org/10.1371/journal.pone.0055319 (2013).
67. Zhang, Y., Liang, X., Lian, Q. & Tse, H. F. Perspective and challenges of mesenchymal stem cells for cardiovascular regeneration. *Expert Rev. Cardiovasc. Ther.* **11**, 505–517. https://doi.org/10.1586/erc.13.5 (2013).
68. Van Pham, P. & Vu, N. B. Production of Clinical-Grade Mesenchymal Stem Cells. In *Stem Cell Processing* (ed. Van Pham, P.) 107–129 (Springer International Publishing, Cham, 2016).
69. Sawangmake, C., Nowwarote, N., Pavasant, P., Chansiripornchai, P. & Osathanon, T. A feasibility study of an in vitro differentiation potential toward insulin-producing cells by dental tissue-derived mesenchymal stem cells. *Biochem. Biophys. Res. Commun.* **452**, 581–587. https://doi.org/10.1016/j.bbrc.2014.08.121 (2014).
70. Sawangmake, C., Rodprasert, W., Osathanon, T. & Pavasant, P. Integrative protocols for an in vitro generation of pancreatic progenitors from human dental pulp stem cells. *Biochem. Biophys. Res. Commun.* **530**, 222–229. https://doi.org/10.1016/j.bbrc.2020.06.145 (2020).
71. Sun, Y. *et al.* Differentiation of bone marrow-derived mesenchymal stem cells from diabetic patients into insulin-producing cells in vitro. *Chin. Med. J. (Engl)* **120**, 771–776 (2007).
72. Al Madhoun, A. *et al.* Defined three-dimensional culture conditions mediate efficient induction of definitive endoderm lineage from human umbilical cord Wharton's jelly mesenchymal stem cells. *Stem Cell Res. Ther.* **7**, 165. https://doi.org/10.1186/s13287-016-0426-9 (2016).
73. D'Amour, K. A. *et al.* Efficient differentiation of human embryonic stem cells to definitive endoderm. *Nat. Biotechnol.* **23**, 1534–1541. https://doi.org/10.1038/nbt1163 (2005).
74. Illing, A. *et al.* Definitive endoderm formation from plucked human hair-derived induced pluripotent stem cells and SK channel regulation. *Stem Cells Int.* **2013**, 360573. https://doi.org/10.1155/2013/360573 (2013).
75. Kunisada, Y., Tsubooka-Yamazoe, N., Shoji, M. & Hosoya, M. Small molecules induce efficient differentiation into insulin-producing cells from human induced pluripotent stem cells. *Stem Cell Res.* **8**, 274–284. https://doi.org/10.1016/j.scr.2011.10.002 (2012).
76. Naujok, O., Diekmann, U. & Lenzen, S. The generation of definitive endoderm from human embryonic stem cells is initially independent from activin A but requires canonical Wnt-signaling. *Stem Cell Rev. Rep.* **10**, 480–493. https://doi.org/10.1007/s12015-014-9509-0 (2014).
77. Teo, A. K., Valdez, I. A., Dirice, E. & Kulkarni, R. N. Comparable generation of activin-induced definitive endoderm via additive Wnt or BMP signaling in absence of serum. *Stem Cell Rep.* **3**, 5–14. https://doi.org/10.1016/j.stemcr.2014.05.007 (2014).
78. Tada, S. *et al.* Characterization of mesendoderm: a diverging point of the definitive endoderm and mesoderm in embryonic stem cell differentiation culture. *Development* **132**, 4363–4374. https://doi.org/10.1242/dev.02005 (2005).
79. Wlizla, M. & Zorn, A. M. Vertebrate Endoderm Formation. In *Principles of Developmental Genetics* (ed. Moody, S. A.) 237–253 (Academic Press, 2015).
80. Choi, S. C. *et al.* Mixl1 and Flk1 are key players of Wnt/TGF-β signaling during DMSO-induced mesodermal specification in P19 cells. *J. Cell Physiol.* **230**, 1807–1821. https://doi.org/10.1002/jcp.24892 (2015).
81. Izumi, N., Era, T., Akimaru, H., Yasunaga, M. & Nishikawa, S. Dissecting the molecular hierarchy for mesendoderm differentiation through a combination of embryonic stem cell culture and RNA interference. *Stem Cells* **25**, 1664–1674. https://doi.org/10.1634/stemcells.2006-0681 (2007).
82. Katsumoto, K. & Kume, S. Endoderm and mesoderm reciprocal signaling mediated by CXCL12 and CXCR4 regulates the migration of angioblasts and establishes the pancreatic fate. *Development* **138**, 1947–1955. https://doi.org/10.1242/dev.058719 (2011).
83. Ulmer, B. *et al.* A novel role of the organizer gene Goosecoid as an inhibitor of Wnt/PCP-mediated convergent extension in Xenopus and mouse. *Sci. Rep.* **7**, 43010. https://doi.org/10.1038/srep43010 (2017).
84. Viotti, M., Nowotschin, S. & Hadjantonakis, A.-K. SOX17 links gut endoderm morphogenesis and germ layer segregation. *Nat. Cell Biol.* **16**, 1146–1156. https://doi.org/10.1038/ncb3070 (2014).
85. Jennings, R. E., Berry, A. A., Strutt, J. P., Gerrard, D. T. & Hanley, N. A. Human pancreas development. *Development* **142**, 3126–3137. https://doi.org/10.1242/dev.120063 (2015).
86. Márquez-Aguirre, A. L., Canales-Aguirre, A. A., Padilla-Camberos, E., Esquivel-Solis, H. & Díaz-Martínez, N. E. Development of the endocrine pancreas and novel strategies for β-cell mass restoration and diabetes therapy. *Braz. J. Med. Biol. Res.* **48**, 765–776. https://doi.org/10.1590/1414-431x20154363 (2015).
87. Caronna, E. A., Patterson, E. S., Hummert, P. M. & Kroll, K. L. Geminin restrains mesendodermal fate acquisition of embryonic stem cells and is associated with antagonism of Wnt signaling and enhanced polycomb-mediated repression. *Stem Cells* **31**, 1477–1487. https://doi.org/10.1002/stem.1410 (2013).
88. Jiang, F.-X. & Morahan, G. Pancreatic stem cells: Unresolved business. *Stem Cells Clin. Res.* https://doi.org/10.5772/23760 (2011).
89. Zaret, K. S. & Grompe, M. Generation and regeneration of cells of the liver and pancreas. *Science* **322**, 1490–1494. https://doi.org/10.1126/science.1161431 (2008).
90. Konagaya, S. & Iwata, H. Chemically defined conditions for long-term maintenance of pancreatic progenitors derived from human induced pluripotent stem cells. *Sci. Rep.* **9**, 640. https://doi.org/10.1038/s41598-018-36606-7 (2019).
91. Cras-Méneur, C., Elghazi, L., Czernichow, P. & Scharfmann, R. Epidermal growth factor increases undifferentiated pancreatic embryonic cells in vitro: A balance between proliferation and differentiation. *Diabetes* **50**, 1571–1579. https://doi.org/10.2337/diabetes.50.7.1571 (2001).
92. Mattin, M. *et al.* An epidemiological study of diabetes mellitus in dogs attending first opinion practice in the UK. *Vet. Rec.* **174**, 349. https://doi.org/10.1136/vr.101950 (2014).
93. Öström, M. *et al.* Retinoic acid promotes the generation of pancreatic endocrine progenitor cells and their further differentiation into β-cells. *PLoS ONE* **3**, e2841. https://doi.org/10.1371/journal.pone.0002841 (2008).
94. Ameri, J. *et al.* FGF2 specifies hESC-derived definitive endoderm into foregut/midgut cell lineages in a concentration-dependent manner. *Stem Cells* **28**, 45–56. https://doi.org/10.1002/stem.249 (2010).
95. Hebrok, M., Kim, S. K. & Melton, D. A. Notochord repression of endodermal Sonic hedgehog permits pancreas development. *Genes Dev.* **12**, 1705–1713. https://doi.org/10.1101/gad.12.11.1705 (1998).
96. McCracken, K. W. & Wells, J. M. Molecular pathways controlling pancreas induction. *Semin. Cell Dev. Biol.* **23**, 656–662. https://doi.org/10.1016/j.semcdb.2012.06.009 (2012).
97. Nostro, M. C. *et al.* Efficient generation of NKX6-1+ pancreatic progenitors from multiple human pluripotent stem cell lines. *Stem Cell Rep.* **4**, 591–604. https://doi.org/10.1016/j.stemcr.2015.02.017 (2015).
98. Gomez, D. L. *et al.* Neurogenin 3 expressing cells in the human exocrine pancreas have the capacity for endocrine cell fate. *PLoS ONE* **10**, e0133862. https://doi.org/10.1371/journal.pone.0133862 (2015).
99. Lee, J. C. *et al.* Regulation of the pancreatic pro-endocrine gene neurogenin3. *Diabetes* **50**, 928–936. https://doi.org/10.2337/diabetes.50.5.928 (2001).

100. Mfopou, J. K., Chen, B., Mateizel, I., Sermon, K. & Bouwens, L. Noggin, retinoids, and fibroblast growth factor regulate hepatic or pancreatic fate of human embryonic stem cells. *Gastroenterology* **138**(2233–2245), 2245.e2231–2214. https://doi.org/10.1053/j.gastro.2010.02.056 (2010).

101. Nostro, M. C. *et al.* Stage-specific signaling through TGFβ family members and WNT regulates patterning and pancreatic specification of human pluripotent stem cells. *Development* **138**, 861–871. https://doi.org/10.1242/dev.055236 (2011).

102. Bendjennat, M. UV irradiation triggers ubiquitin-dependent degradation of p21(WAF1) to promote DNA repair. *Cell* **114**, 599–610. https://doi.org/10.1016/j.cell.2003.08.001 (2003).

103. Jara, C. *et al.* Microencapsulation of cellular aggregates composed of differentiated insulin and glucagon-producing cells from human mesenchymal stem cells derived from adipose tissue. *Diabetol. Metab. Syndr.* **12**, 66. https://doi.org/10.1186/s13098-020-00573-9 (2020).

104. Legøy, T. A. *et al.* Encapsulation boosts islet-cell signature in differentiating human induced pluripotent stem cells via integrin signalling. *Sci. Rep.* **10**, 414. https://doi.org/10.1038/s41598-019-57305-x (2020).

105. Richardson, T., Kumta, P. N. & Banerjee, I. Alginate encapsulation of human embryonic stem cells to enhance directed differentiation to pancreatic islet-like cells. *Tissue Eng. Part A* **20**, 3198–3211. https://doi.org/10.1089/ten.TEA.2013.0659 (2014).

106. Liu, H. *et al.* A droplet microfluidic system to fabricate hybrid capsules enabling stem cell organoid engineering. *Adv. Sci.* **7**, 1903739. https://doi.org/10.1002/advs.201903739 (2020).

107. Hermansen, K. Forskolin, an activator of adenylate cyclase, stimulates pancreatic insulin, glucagon, and somatostatin release in the dog: Studies in vitro. *Endocrinology* **116**, 2251–2258. https://doi.org/10.1210/endo-116-6-2251 (1985).

108. Leech, C. A. *et al.* Molecular physiology of glucagon-like peptide-1 insulin secretagogue action in pancreatic β cells. *Prog. Biophys. Mol. Biol.* **107**, 236–247. https://doi.org/10.1016/j.pbiomolbio.2011.07.005 (2011).

109. Wan, Q. F. *et al.* Protein kinase activation increases insulin secretion by sensitizing the secretory machinery to Ca2+. *J. Gen. Physiol.* **124**, 653–662. https://doi.org/10.1085/jgp.200409082 (2004).

110. Aoyagi, K. *et al.* Acute inhibition of PI3K-PDK1-Akt pathway potentiates insulin secretion through upregulation of newcomer granule fusions in pancreatic β-cells. *PLoS ONE* **7**, e47381. https://doi.org/10.1371/journal.pone.0047381 (2012).

111. Adams, M. T., Gilbert, J. M., Hinojosa Paiz, J., Bowman, F. M. & Blum, B. Endocrine cell type sorting and mature architecture in the islets of Langerhans require expression of Roundabout receptors in β cells. *Sci. Rep.* **8**, 10876. https://doi.org/10.1038/s41598-018-29118-x (2018).

112. Piccand, J. *et al.* Rfx6 maintains the functional identity of adult pancreatic β cells. *Cell Rep.* **9**, 2219–2232. https://doi.org/10.1016/j.celrep.2014.11.033 (2014).

113. Thorens, B. GLUT2, glucose sensing and glucose homeostasis. *Diabetologia* **58**, 221–232. https://doi.org/10.1007/s00125-014-3451-1 (2015).

114. Hwang, Y., Cha, S. H., Hong, Y., Jung, A. R. & Jun, H. S. Direct differentiation of insulin-producing cells from human urine-derived stem cells. *Int. J. Med. Sci.* **16**, 1668–1676. https://doi.org/10.7150/ijms.36011 (2019).

115. Liu, X. *et al.* Enhanced differentiation of human pluripotent stem cells into pancreatic endocrine cells in 3D culture by inhibition of focal adhesion kinase. *Stem Cell Res. Ther.* **11**, 488. https://doi.org/10.1186/s13287-020-02003-z (2020).

116. Xu, B. *et al.* Three-dimensional culture promotes the differentiation of human dental pulp mesenchymal stem cells into insulin-producing cells for improving the diabetes therapy. *Front. Pharmacol.* **10**, 1576–1576. https://doi.org/10.3389/fphar.2019.01576 (2020).

117. Yang, S. F. *et al.* Nicotinamide facilitates mesenchymal stem cell differentiation into insulin-producing cells and homing to pancreas in diabetic mice. *Transpl. Proc.* **47**, 2041–2049. https://doi.org/10.1016/j.transproceed.2015.05.019 (2015).

118. Kojayan, G. G., Flores, A., Li, S., Alexander, M. & Lakey, J. R. T. Cryopreserved alginate-encapsulated islets can restore euglycemia in a diabetic animal model better than cryopreserved non-encapsulated islets. *Cell Med.* **11**, 2155179019876641. https://doi.org/10.1177/2155179019876641 (2019).

119. Liu, Q. *et al.* Zwitterionically modified alginates mitigate cellular overgrowth for cell encapsulation. *Nat. Commun.* **10**, 5262. https://doi.org/10.1038/s41467-019-13238-7 (2019).

120. Westenfelder, C., Gooch, A., Hu, Z., Ahlstrom, J. & Zhang, P. Durable control of autoimmune diabetes in mice achieved by intraperitoneal transplantation of "Neo-islets", three-dimensional aggregates of allogeneic islet and "mesenchymal stem cells". *Stem Cells Transl. Med.* **6**, 1631–1643. https://doi.org/10.1002/sctm.17-0005 (2017).

121. Hoeferlin, L. A., Oleinik, N. V., Krupenko, N. I. & Krupenko, S. A. Activation of p21-dependent G1/G2 arrest in the absence of DNA damage as an antiapoptotic response to metabolic stress. *Genes Cancer* **2**, 889–899. https://doi.org/10.1177/1947601911432495 (2011).

122. Ock, S. A., Knott, J. G. & Choi, I. Involvement of CDKN1A (p21) in cellular senescence in response to heat and irradiation stress during preimplantation development. *Cell Stress Chaperones* **25**, 503–508. https://doi.org/10.1007/s12192-020-01090-4 (2020).

123. El Idrissi, A., Boukarrou, L. & L'Amoreaux, W. Taurine supplementation and pancreatic remodeling. *Adv. Exp. Med. Biol.* **643**, 353–358 (2009).

124. Woodford, C. *et al.* Nicotinamide promotes differentiation of pancreatic endocrine progenitors from human pluripotent stem cells through poly (ADP-ribose) polymerase inhibition. *bioRxiv*, 2020.2004.2021.052951. https://doi.org/10.1101/2020.04.21.052951 (2020).

125. Castaing, M., Duvillié, B., Quemeneur, E., Basmaciogullari, A. & Scharfmann, R. Ex vivo analysis of acinar and endocrine cell development in the human embryonic pancreas. *Dev. Dyn.* **234**, 339–345. https://doi.org/10.1002/dvdy.20547 (2005).

126. Ikemoto, T. *et al.* In vitro and in vivo effects of insulin-producing cells generated by xeno-antigen free 3D culture with RCP piece. *Sci. Rep.* **9**, 10759. https://doi.org/10.1038/s41598-019-47257-7 (2019).

127. Kroon, E. *et al.* Pancreatic endoderm derived from human embryonic stem cells generates glucose-responsive insulin-secreting cells in vivo. *Nat. Biotechnol.* **26**, 443–452. https://doi.org/10.1038/nbt1393 (2008).

128. Ma, H., Wert, K. J., Shvartsman, D., Melton, D. A. & Jaenisch, R. Establishment of human pluripotent stem cell-derived pancreatic β-like cells in the mouse pancreas. *Proc. Natl. Acad. Sci. U.S.A.* **115**, 3924–3929. https://doi.org/10.1073/pnas.1702059115 (2018).

129. Rezania, A. *et al.* Maturation of human embryonic stem cell-derived pancreatic progenitors into functional islets capable of treating pre-existing diabetes in mice. *Diabetes* **61**, 2016–2029. https://doi.org/10.2337/db11-1711 (2012).

130. Shahjalal, H. M. *et al.* Generation of insulin-producing β-like cells from human iPS cells in a defined and completely xeno-free culture system. *J. Mol. Cell Biol.* **6**, 394–408. https://doi.org/10.1093/jmcb/mju029 (2014).

131. Agulnick, A. D. *et al.* Insulin-producing endocrine cells differentiated in vitro from human embryonic stem cells function in macroencapsulation devices in vivo. *Stem Cells Transl. Med.* **4**, 1214–1222. https://doi.org/10.5966/sctm.2015-0079 (2015).

132. Rezania, A. *et al.* Reversal of diabetes with insulin-producing cells derived in vitro from human pluripotent stem cells. *Nat. Biotechnol.* **32**, 1121–1133. https://doi.org/10.1038/nbt.3033 (2014).

133. Russ, H. A. *et al.* Controlled induction of human pancreatic progenitors produces functional beta-like cells in vitro. *Embo J.* **34**, 1759–1772. https://doi.org/10.15252/embj.201591058 (2015).

134. Choudhury, A. R. *et al.* Cdkn1a deletion improves stem cell function and lifespan of mice with dysfunctional telomeres without accelerating cancer formation. *Nat. Genet.* **39**, 99–105. https://doi.org/10.1038/ng1937 (2007).

135. Sarmadi, V. H. *et al.* Human mesenchymal stem cells-mediated transcriptomic regulation of leukemic cells in delivering anti-tumorigenic effects. *Cell Transpl.* **29**, 0963689719885077. https://doi.org/10.1177/0963689719885077 (2020).

136. Velasco-Velázquez, M. A., Yu, Z., Jiao, X. & Pestell, R. G. Cancer stem cells and the cell cycle: Targeting the drive behind breast cancer. *Expert Rev. Anticancer Ther.* **9**, 275–279. https://doi.org/10.1586/14737140.9.3.275 (2009).

137. Azzarelli, R. *et al.* Multi-site neurogenin3 phosphorylation controls pancreatic endocrine differentiation. *Dev. Cell* **41**, 274-286. e275. https://doi.org/10.1016/j.devcel.2017.04.004 (2017).

138. Sawangmake, C., Pavasant, P., Chansiripornchai, P. & Osathanon, T. High glucose condition suppresses neurosphere formation by human periodontal ligament-derived mesenchymal stem cells. *J. Cell Biochem.* **115**, 928–939. https://doi.org/10.1002/jcb.24735 (2014).

139. Asadi, A., Bruin, J. E. & Kieffer, T. J. Characterization of antibodies to products of proinsulin processing using immunofluorescence staining of pancreas in multiple species. *J. Histochem. Cytochem.* **63**, 646–662. https://doi.org/10.1369/0022155415576541 (2015).

140. Harrington, S. *et al.* Improved yield of canine islet isolation from deceased donors. *BMC Vet. Res.* **13**, 264. https://doi.org/10.1186/s12917-017-1177-2 (2017).

Acknowledgements

Author contributions

Q.D.L. performed most of the experiments; collected, analyzed, and interpreted the data; and wrote the manuscript. W.R. edited the manuscript and supported the ideas. S.K. provided the discussion and instructed the encapsulation protocol. P.P. and T.O. conceived the main ideas and approved the final manuscript. C.S. conceived the main ideas, designed the experiments, analyzed and interpreted the data, and wrote and approved the final manuscript.

Competing interests

The authors declare no competing interests.

Additional information

Supplementary Information The online version contains supplementary material available at https://doi.org/10.1038/s41598-022-13114-3.

Correspondence and requests for materials should be addressed to C.S.

Reprints and permissions information is available at www.nature.com/reprints.

Publisher's note Springer Nature remains neutral with regard to jurisdictional claims in published maps and institutional affiliations.